infrastructures

MDPI

Review

Geopolymers: The Green Alternative to Traditional Materials for Engineering Applications

Zahraa Jwaida [1], Anmar Dulaimi [2,3,*], Nuha Mashaan [4,*] and Md Azree Othuman Mydin [5]

[1] Industrial Preparatory School of Vocational Education Department, Educational Directorate Babylon, Ministry of Education, Babylon 51001, Iraq; zhraengineer@gmail.com
[2] College of Engineering, University of Warith Al-Anbiyaa, Ministry of Education, Karbala 56001, Iraq
[3] School of Civil Engineering and Built Environment, Liverpool John Moores University, Liverpool L3 2ET, UK
[4] School of Engineering, Edith Cowan University, Joondalup, WA 6027, Australia
[5] School of Housing, Building and Planning, Universiti Sains Malaysia, Penang 11800, Malaysia; azree@usm.my
* Correspondence: a.f.dulaimi@uowa.edu.iq (A.D.); n.mashaan@ecu.edu.au (N.M.)

Abstract: Researchers have been driven to investigate sustainable alternatives to cement production, such as geopolymers, due to the impact of global warming and climate change resulting from greenhouse gas emissions. Currently, they are exploring different methods and waste materials to enhance the mechanical and physical properties of geopolymer and expand its application range. This review paper offers a thorough analysis of the utilization of various waste materials in geopolymer manufacturing and shows the creative contribution of this research to the development of environmentally friendly cement substitutes. The article covers the properties, durability, and practical applications of geopolymer composites made from various waste binders. It includes a microstructure and chemical analysis. The research findings indicate that geopolymers are an effective cementitious binder substitute for cement in various applications. Additionally, the ecological and carbon footprint analysis highlights the sustainability of geopolymers compared to cement.

Keywords: geopolymer; waste materials; review; sustainability

Citation: Jwaida, Z.; Dulaimi, A.; Mashaan, N.; Othuman Mydin, M.A. Geopolymers: The Green Alternative to Traditional Materials for Engineering Applications. *Infrastructures* **2023**, *8*, 98. https://doi.org/10.3390/infrastructures8060098

Academic Editor: Ali Behnood

Received: 16 April 2023
Revised: 8 May 2023
Accepted: 20 May 2023
Published: 23 May 2023

1. Introduction

For the development of a country, the construction industry has a significant role, accounting for more than 6% of the gross domestic product globally [1]. The development of infrastructure and urbanization require producing considerable amounts of concrete. Cement represents a main constituent of concrete which binds filler and aggregate materials.

Cement mainly consists of silicon, calcium, and aluminum and minerals such as iron ore, chalk, clay, and limestone [2], which are mined or quarried from natural resources. Moreover, during the manufacturing of cement, the required fossil fuels such as coal and petroleum are also considered natural resources. The energy required for the manufacturing also includes that needed for the grinding and heating of raw materials to more than 1450 °C. Additionally, the thermal decomposition of limestone emits greenhouse gases directly into the atmosphere, including carbon dioxide (CO_2) [3,4], with small quantities of other toxic gases such as sulfur dioxide (SO_2) and nitrogen dioxide (NO_2) [4].

The production of cement is considered a significant contributor to the emissions of carbon dioxide (CO_2). From 2015 to 2020, each ton of cement produced increased CO_2 emissions by 1.8% annually. It was also estimated that about a 3% reduction of CO_2 is needed to achieve net zero emissions by 2050 [5]. It is estimated that the process of cement production causes 4–10% of CO_2 emissions globally [6,7]. During the use of electric power, combustion of fuel, and the process of calcination, each ton of cement produced emits about 0.66–1.5 tons of CO_2 depending on the production system and technique [8,9]. Each ton of cement produced requires 3.2–6.3 GJ of energy and 2.65–2.8 tons of raw materials [10,11]. In addition, dust is generated during cement production which contributes to industrial air

pollution [12]. Thus, reducing the manufacturing of cement reduces the amount of CO_2 emission. With the increasing need for concrete for infrastructure and housing, cement production is increasing daily. It was estimated that about 4100 million metric tons of cement were produced worldwide in 2018 [13]. It was reported by Schneider et al. [14] that the production of cement will increase in 2050 to 4.38 billion tons due to the increasing global demand. In addition, Müller and Harnisch [15] expected a cement production of 5 billion tons in 2030. Such predictions are alarming as the production of cement requires a substantial quantity of energy and raw materials, reducing the available non-renewable fossil fuel and natural resources [12,16].

On the other hand, significant amounts of solid waste are produced by municipalities, agriculture, and industry due to the increasing global population. The amount of discharged waste was estimated at 10.4 billion tons in 2010 and will rise to 148 billion tons by 2025 [17,18]. Although solid wastes can be dealt with by various methods such as decomposition, crushing, incineration, and gasification [19], residues result which cause secondary pollution [17]. Thus, effective reusing or recycling of the residues can minimize the burdens on the environment [20]. With the consideration of the adverse effect of utilizing and producing cement, various researchers have attempted to provide solutions for sustainable technologies. Some of the suggested approaches are to use supplementary cementitious materials (SCMs) to partially replace cement and chemical additives for reducing the consumption of water, usage of alternative fuels, an effective system of cement production, and use of water and recycled materials and concrete [21–24].

Geopolymer binders use by-products such as ground granulated blast furnace slag (GGBS) and fly ash with minimal emission of greenhouse gases from the production of alkali activators. By-product materials have been used in concrete only as a partial replacement since they need to react with the cement hydration product to form binding materials. Thus, there has been substantial interest in developing alternatives that can reduce the dependence on cement while providing approximately similar engineering properties to cement. Geopolymer represents a new binding material that can be produced from the activation of aluminosilicate material with alkaline solutions [4,25]. Thus, geopolymer binders were proposed as an effective solution to fully or partially replace the use of cement. It is estimated by Davidovits [26] that only 0.15 to 0.20 tons of cement are produced from each ton of geopolymer, significantly lower than when using cement alone. This shows the effective potential of replacing cement with geopolymers as an environmentally friendly alternative. Geopolymers have been considered a sustainable solution and eco-friendly disposal of industrial by-product materials such as ground granulated blast furnace slag (GGBS) [27–30], fly ash [28,31–34], metakaolin [34–36], bottom ash [27,35,37], and rice husk ash [27,33,38].

This paper aims to critically review the recent use of geopolymers as an alternative to cement in various fields. The focus of this paper is to provide a comprehensive review of the various usages and incorporations of waste and by-product materials in geopolymer binders for various applications. The use of various by-products including basic geopolymer precursors and other recent alternatives was explored. It was found that important review studies have been conducted on the material properties and the impact of various parameters on the performance and engineering properties of geopolymer binders. However, most of the reviews focused on geopolymer concrete, and little attention was paid to the use of geopolymers in other applications. Moreover, this paper covers additional relevant study publications that were not covered in prior review articles and were recently published. Therefore, this research summarizes and presents a state-of-the-art review of all recent and current research for the use of various waste and by-product materials as geopolymer precursors. Based on the knowledge of the authors, this is the first review paper that combines the various studies on geopolymers in engineering applications. It comprises a systematic review, analysis, and discussion to help researchers and the construction industry obtain a better understanding of the topic. The paper is divided into several sections. The first section deals with general information about geopolymer, its

formation, process, and chemical reactions. The second section focuses on the constituents of geopolymers. The third section presents the mix design and process and curing regime. The results and main finding of the studies are presented in the fourth section while the fifth section focuses on the sustainability of geopolymers in terms of carbon and ecological footprints. The gap between knowledge and future research is also proposed.

2. Geopolymers

In 1976, this alkali-activated material was defined by Joseph Davidovits [39]. Alkali-activated material (AAM) represents an effective alternative to cement due to its better performance and lower environmental impacts. Although the concept of alkali-activated material and geopolymer technology has been widely explored over recent decades, no consensus has been reached for distinguishing between the terminologies [24]. However, according to Provis and Bernal [40], AAM is the widest classification, referring to any system of an aluminosilicate-rich precursor with either no or high calcium content and activated by alkaline activators, whereas geopolymers are a subset of AAM, referring to a system of high aluminosilicate and low calcium content with the presence of alkaline activators [41,42].

Geopolymer is a term for a binder produced from the chemical reactions of a precursor containing silica with alumina material by the presence of alkaline activators. The main components are the source materials which should be rich in major constituents, such as silicon (Si) and aluminum (Al), from either natural or waste and by-product materials, such as clays, kaolinite, etc. or red mud, fly ashes, slags, etc. The liquid is usually based on sodium (hydroxide or silicate) or potassium (hydroxide or silicate) [41,42].

Initially, geopolymer binders were produced as amorphous and inorganic material for their non-combustible, inflammable, and heat-resistant properties for reducing the fire risks of the use of plastic materials in the 1970s in Europe. Then, the use of geopolymer binders was shifted to structural engineering since promising results were obtained by different studies in terms of their behavior and potential of replacing cement [12,43]. Alternative names for geopolymers were also introduced, including geocement, alkali-bonded ceramics and hydroceramics, aluminosilicate inorganic polymers (AIPs), inorganic polymers (IPs), inorganic phosphate cement (IPC), and alkali-activated materials (AAMs), based on the composition and formulation [12,42].

Geopolymer binders are innovative cement-based materials that can substitute OPC composites while emitting less CO_2 than OPC [44]. The desired goal of studies about geopolymer binders in industry and academia has been to obtain an effective alternative to cement. Thus, based on traditional cement-related techniques and science, development and synthesis processes were aligned and evaluated. However, the synthesis and chemistry processes of geopolymers and cement are different due to the different natures of materials and constituents. The binders of cement are synthesized depending on the hydration reactions of silicon dioxide and calcium oxide to produce calcium silicate hydrates (C-S-H) [45,46].

On the other hand, the structure of geopolymer binders as inorganic polymers consists of chained repetitive elements called monomers, controlling the characteristics of geopolymers. The structure is made of sialate (of silico-oxo-aluminate) or alkali aluminosilicate gel with alumina (Al) or silica (Si) ions, presenting alumina and silica bonding by a bridge of oxygen. Geopolymer has an amorphous microstructure similar to a crystalline structure, which allows the reaction with other materials to form binders, while the composition is similar to natural zeolite [45,47]. Van Jaarsveld et al. [48] found that the crystalline and amorphous degree in fly-ash-based geopolymers is a key parameter impacting the mechanical and physical characteristics.

According to Davidovits [26], the term polysialate is used to chemically designate aluminosilicate-based geopolymers, while sialate is the abbreviation for silico-oxo-aluminate (Si-O-Al-O) [49]. The process of geopolymerization involves the chemical reaction of aluminosilicate oxide minerals with a high-alkaline solution. The process is a very fast reaction and, during the process, the geopolymer blocks are created by polymeric bonds and

three-dimensional sialate (Si-O-Al-O) chained structures [50,51]. The quantity of alumina and silica in the structure impacts the degree of reaction and bonding and thereby the characteristics of geopolymers. The following formula represents the created polysialate chained structure:

$$M_n\ [-(SiO_2)_z\text{-}AlO_2)]n.wH_2O$$

where M is a cation or alkaline element (e.g., potassium, sodium, etc.), z is a value of 1–3 or higher depending on the reaction chemistry, n is the polymerization degree, w is the hydration degree [39]. The polysialate formation and its chemical structure are illustrated in Figure 1 as depicted by Davidovits [26]. The polysialate structure depends on the spatial arrangement and organization of alternately linked SiO_4 and AlO_4 with all shared oxygen ions, which can form several repeating units (monomers).

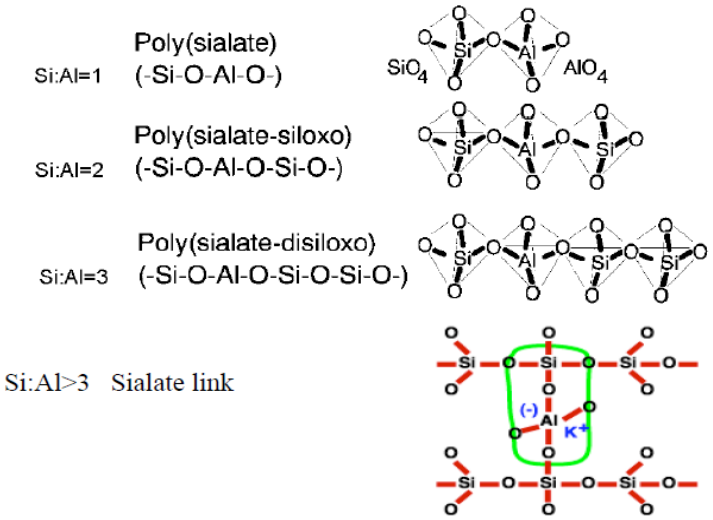

Figure 1. The polysialate formation of geopolymerization process [26].

However, the geopolymerization mechanism is not thoroughly understood due to the existence of influential parameters in the process. Various studies indicated that the process consists of three main stages: dissolution and destruction of alumina and silica ions from precursors by hydrolysis of alkaline activators, the re-orientation and transportation of cation ions into monomers, and polycondensation of the monomers into polymeric structures. The stages can overlap with each other and therefore are difficult to study or isolate [12,52–54].

In the 1950s, alkaline-activated mechanisms were first explored by Glukhovsky, who divided the process into three phases: destruction–coagulation; coagulation–condensation; condensation–crystallization [42]. Later on, researchers such as Shi et al. [51], Fernandez-Jimenez et al. [55], and Duxson et al. [56] reviewed the Glukhovsky model and proposed a new model for the geopolymerization process, as shown in Figure 2. Figure 3 illustrates the chemical reactions of geopolymerization [57–59]. Alkaline activators dissolve aluminosilicate materials into silicate and aluminum ions (AlO_4 and SiO_4 tetrahedral units) with a pH greater than 10. Aluminosilicate gel is formed by the shift of the ions to an equilibrium state and then interaction. A small degree of structural order is observed, which favors a stable Al-rich compound. Silicon and aluminum tetrahedrons join, producing rings with four secondary tetrahedral units [55]. The high concentration of aluminum in the precipitation of gel 1 (SiAl = 1) results from the significant concentration of Al + 3 ions in the alkaline medium at the beginning of the reaction [40,60]. Firstly, the gel consists of alumina since it dissolves faster than alumina, then following the dissolution of silicate, the gel is said to be a zeolite precursor gel. This gel is more stable than aluminum gel due to stronger SiO bonds than Al-O bonds [61]. More Si–O bonds are broken from the precursors as the reaction progresses, which dissolve and thereby increase the concentration of silicon in

the solution, reaching the gel 2 precipitation model (SiAl = 2). This rise in the ratio of Si/Al ratio improves the mechanical characteristics of the formed aluminosilicate gels [62]. Finally, the formation of an amorphous to semi-crystalline aluminosilicate network is developed with the desired physical characteristics. The final products are based on the characteristics of alkaline activators and source materials and the contents of calcium, aluminosilicate, or magnesium. Such products can be sodium aluminosilicate hydrate (N-A-S-H) (Na + Al + Si), polymers or zeolite from alumina or silica, or C-S-H gel [61,63,64]. The existence of alumina, silica, and calcium species can produce aluminosilicate hydrate (C-A-S-H) gel products, which can often be seen in GGBS geopolymer binders. In terms of the secondary products, in addition to the formation of the C-S-H gel inside the material, they include portlandite, ettringite, and calcium monosulfoaluminate [41,65].

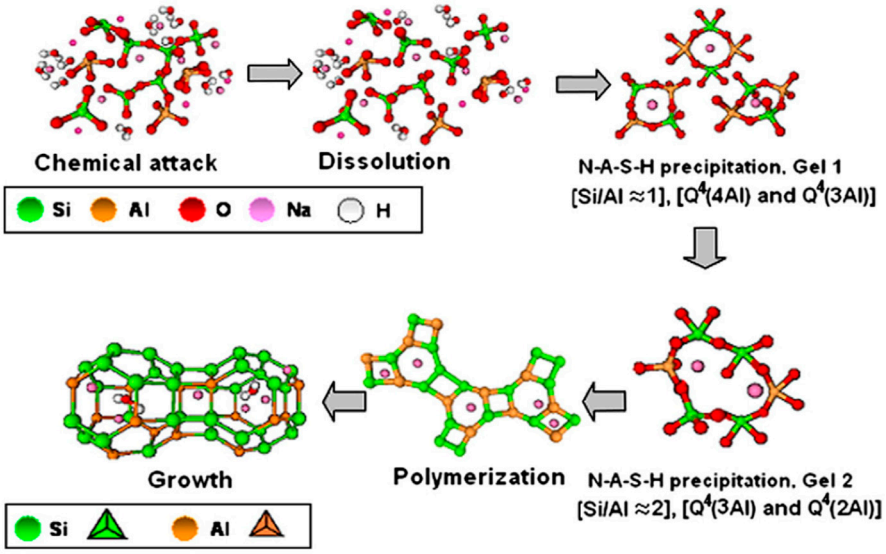

Figure 2. Stages of geopolymerization process [54].

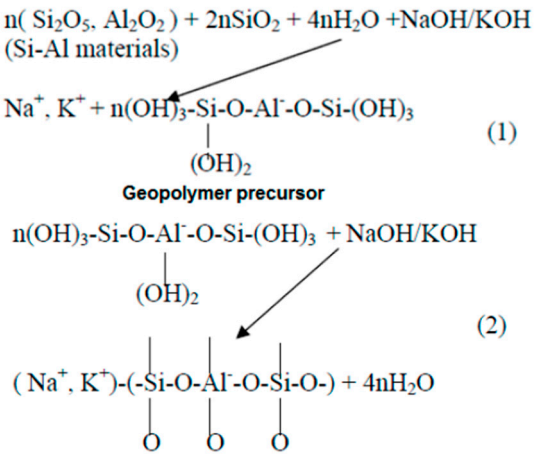

Figure 3. Reactions during geopolymerization [59]. (1) Dissolution of Si and Al atoms from the source material through the action of hydroxide ions, (2) Transportation or orientation or condensation of precursor ions into monomers followed by Setting or polycondensation/polymerisation of monomers into polymeric structures.

Additionally, water (H_2O) is a product of the process indicated by the proposed model, chemical reactions, and the formulation of the polysialate chain structure. Hardjito and Rangan [47] mentioned that chemically free water resulted during the chemical reactions of the process from the matrix of the geopolymer and was removed in the drying and curing steps. However, the role of water is negligible in comparison with the hydration process

of cement, though it impacts the workability and produces micro- and nanovoids in the matrix [66]. Since water lacks involvement in the process, the properties and microstructure binders are influenced by the ingress water resistance, elevated temperatures, chemical attacks, and alkali-aggregate reactivity [67].

When the amount of activator is lower than required, some of the aluminosilicate precursors do not undergo a reaction due to the lack of reaction medium. Low dissolution of aluminosilicate does not cause a change in the setting time. In addition, various researchers [68,69] reported that the geopolymer structure is similar to zeolites, though the geopolymer has denser mesoporous and semi-crystalline or amorphous structures in comparison with the crystalline structure of zeolites [70,71]. This could result from the vast dissolution of the glassy constituents during the mixing of the alkali activators with the precursors. In this case, space and time are not adequate for the growth of the gel into a well-crystallized structure, forming semi-crystalline, amorphous, or microcrystalline structures [72].

Studies have indicated that the content of active calcium in the raw materials determines the nanostructures of geopolymers. A highly crosslinked zeolite-like N-A-S-H structure is formed with a low amount of active calcium, with Q4 (4Al) as the main units of the structure [73,74]. With the presence of humidity, oligomeric aluminum-rich colloids are formed by the rapid combination of aluminum–oxygen and silicon–oxygen tetrahedrons. In contrast, the polymerization degree of aluminum-rich colloids is low with low levels of humidity. With a high content of calcium, C-A-S-H gel is formed, similar to tobermorite in structure. N-A-S-H and C-A-S-H can both occur in the system, though at high pH levels of more than 12, the N-A-S-H is slowly transformed into C-A-S-H [75].

2.1. Components of Geopolymers

2.1.1. Aluminosilicate (AS)

This includes the main precursors with various materials that have been utilized to produce geopolymer binders. Of those, the main sources of alumina silicate which have been widely used include ground granulated blast furnace slag (GGBS), fly ash (FA), and metakaolin (MK). These are explored in detail below.

(1) Fly ash (FA)

FA is created by power plants and in some industries by steam or electric generation centers. In general, after crushing and placing coal in an ignition chamber in the presence of air, it undergoes impulsive sparking, generating mineral traces and heat. In the kiln, the heat is eradicated by broiler tubes, cooling the flue gas with the formation of hardened mineral residues. Fly ash particles are retained in the flue gas while coarser ash is present in the chamber and known as slag. The use of fabric filters or electrostatic precipitators for the culmination process for controlling particulate emissions allows the collection of the FA. The ash mainly contains alumina and silica, which assist in forming cement as a substitute. With the presence of water, FA reacts with lime to form similar compounds to cement [7,76].

FA has been widely reported as a building material with various applications in concrete, mortars, and pastes [73,77]. Additionally, it has been reported that about 1000 million tonnes of FA are produced worldwide annually, which is undesirable from the environmental aspect. It functions as a binder in the geopolymer with the presence of an alkaline activator. Figure 4 illustrates a scanning electron microscope (SEM) image and X-ray diffraction (XRD) graph of FA [7,78]. The SEM image shows the particles of ash have a spherical shape which permits their easy mixing and flow in the mixtures. The XRD peak indicates the existence of an amorphous phase of the FA, with a late reaction with the hydration products. The existence of crystalline impurities in the FA is indicated by the sharp peaks of the XRD graph.

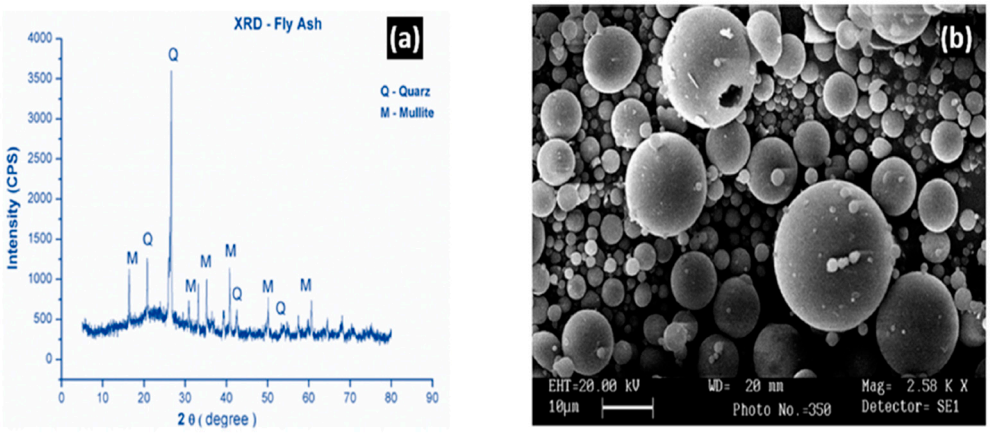

Figure 4. (**a**) XRD and (**b**) SEM of FA [7,78].

The ash is often used as a replacement for cement in the production of concrete [79], with higher durability and strength in comparison with traditional concrete [7]. Its lower costs and sulfate resistance mainly contribute to its use in cement replacement [80]. The use of ash represents a sustainable solution to environmental issues since it reduces the required amount of energy and water in cement production, causes relatively lower CO_2 emissions, and conserves landfilling areas [81]. The use of 1000 Kg of FA can cut the CO_2 emission by 1000 Kg. The use of all annually produced amounts of FA equals the prevention of 25% of CO_2 released through vehicles globally [82]. FA has wide applications, therefore it plays a significant role in the green and economic application of technologies. It has been used in soil stabilization [83,84], zeolite production [85], and retrieval of nutrients [86].

(2) Ground Granulated Blast Furnace Slag (GGBS)

GGBS is a by-product of steel and iron production in blast furnaces in which coke, calcium carbonate ($CaCO_3$), and iron ore are heated at about 1500 °C. Molten slag and iron are produced as a result of material softening in the blast furnace. High-strain water is applied to the molten slag floating above the molten iron to obtain granular particles. Then, the particles are dehydrated and ground to fine materials to create the GGBS product [29]. The product is a renowned building material, widely used in the production of concrete, mortar, and cement [87]. The particles of GGBS have a glassy structure and contain monosilicate, similar to cement clinker [88]. As a replacement for cement, GGBS has been used for increasing heat generation in the hydration process, resistance to sulfate, strength, and reducing permeability and water demands [79]. Thus, it can be effectively used in geopolymers. Figure 5 illustrates the SEM and XRD of GGBS [89]. The SEM image indicates the irregular shape of the particles and the amorphous nature of the materials, indicating the reactivity of GGBS in comparison with FA. The XRD peak confirms the higher reactivity of GGBS. The blending of GGBS can enhance the cementitious property of the cement though negatively impacting the flow characteristics due to the irregular shape of the particles [76].

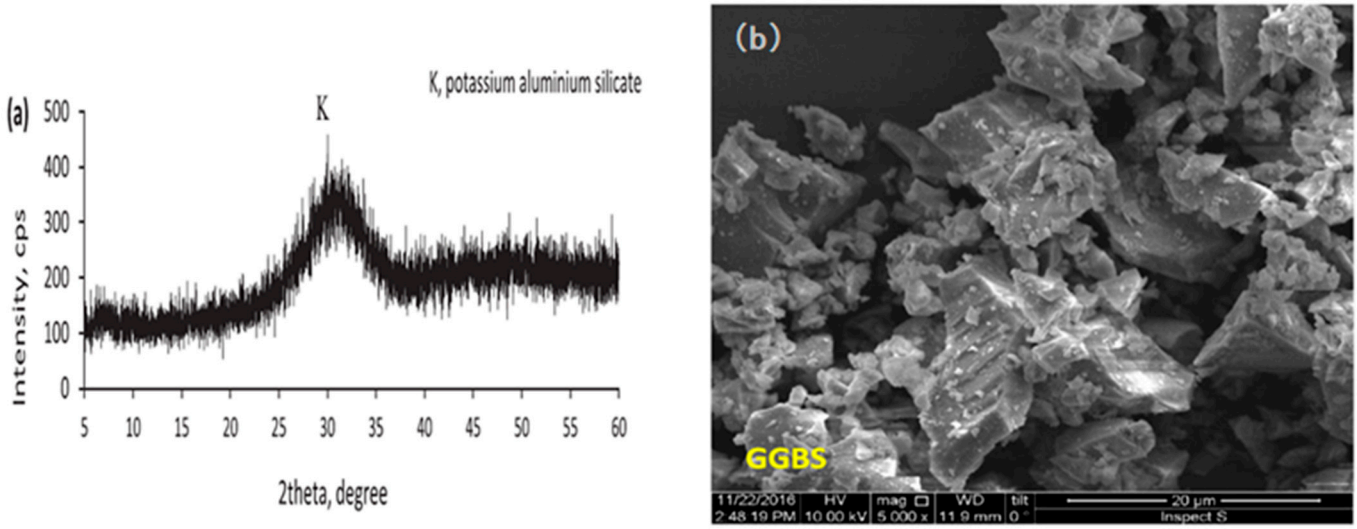

Figure 5. (**a**) XRD and (**b**) SEM of GGBS [89].

(3) Metakaolin (MK)

Metakaolin derived from the name of a Chinese city (Gaoling) in Jiangxi Province, southeast China. MK is also known as China clay. Scientifically, it is a rock with a substantial amount of kaolinite ($Al_2Si_2O_5(OH)_4$). It consists of layers of octahedral sheets of alumina (Al (O, $OH)_6$) linked to tetrahedral sheets of silica (SiO_4), sharing the atoms of oxygen. It has been widely used in ceramic and paper production, paints and rubber filler, and mortar and concrete for increasing the strength and durability of cementitious paste. Around 25.7 million tonnes of kaolin was produced in 2011 according to the British Geological Survey with the main producers being the US, Germany, China, Brazil, Korea, and Iran, contributing to about 75% of the total production [90,91]. This shows the significant potential of MK to be used in geopolymers. Figure 6 shows a SEM image and XRD graph of MK [90,92], indicating the existence of an aluminosilicate composite with semi-crystalline phases. The SEM image indicates a plate-like structure that assists in the geopolymerization process. The XRD graph indicates peaks of quartz and muscovite with a range of 10 to 70.

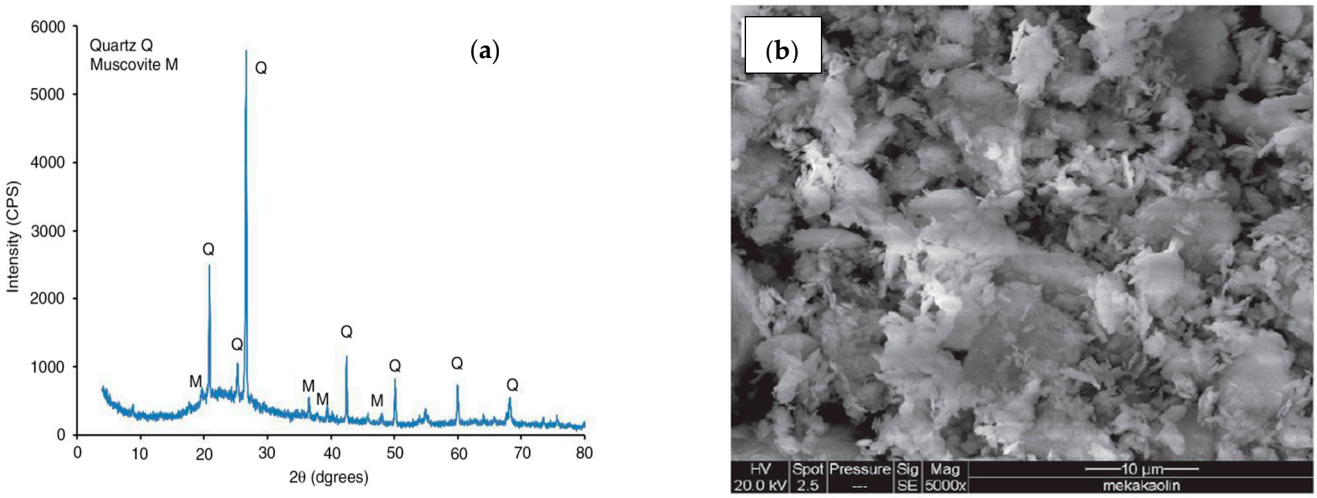

Figure 6. (**a**) XRD and (**b**) SEM of MK [90,92].

(4) Alternative precursors

Any material rich in alumina and silica can be used as a precursor for geopolymer binders. Thus, when checking waste and by-products materials, their chemical composi-

tions should be investigated [29,93]. Natural minerals such as bentonite, mullite, halloysite, diatomite, bauxite, etc. can also be used as precursors though they require the use of high-temperature pretreatment for sufficient activity due to their low amorphous contents. Construction and demolition wastes such as brick wastes and crushed waste glass have also been explored by various researchers for use in geopolymer concrete to reduce the amount of cement or aggregates. In addition, adding recycled waste can help reduce waste and protect natural resources [94]. For the various reviewed studies in this paper, the chemical compositions of some of the explored waste and by-product materials other than basic precursors are shown in Table 1. These include drinking water treatment sludge (DWTS), silica fume (SF), mine tailings (MTs), activated tailings (ATs), spent fluid catalytic cracking (SFCC), sewage sludge ash (SSA), nanoparticles (NPs), corncob ash (CCA), waste glass powder (WGP), cow bone ash (CBA), lime kiln dust (LKD), fluid catalytic cracking (FCC), palm oil fuel ash (POFA), brick powder (BP), plant ash (PA), and recycled asphalt pavement (RAP). These materials have been synthesized for usage in geopolymer binders with compressive strength ranging from 40 to 85 MPa [58,95]. The materials can be used separately or blended with basic precursors such as FA, GGBS, and MK. As indicated in the table, the materials are reported to have adequate amounts of alumina and silica, and the content of calcium oxide cannot be ignored. This suggests their potential for application in geopolymers. The presence of such materials can variably impact the tension performance and properties of the resultant geopolymers. The effective raw materials should have amorphous characteristics and an outstanding ability to easily release aluminum [95].

Table 1. Chemical compositions of alternative precursors.

Reference	Material Type	Chemical Composition							
		SiO_2	Al_2O_3	CaO	Fe_2O_3	MgO	Na_2O	SO_3	TiO_2
[96]	DWTS	33.07	48.21	2.94	6.74	1.48	0.28	1.70	0.51
[97]	SF	96.9	0.15	0.53	0.06	1.10	-	0.12	-
[98]	MTs ATs	70.29	16.12	1.79	1.31	0.38	3.35	0.16	0.17
[99]	SFCC	37.63	55.29	0.84 (CeO_2)	0.58	-	0.15	-	-
[100]	SSA	44.40	15.14	18.75	7.86	3.00	1.96	3.01	0.91
[67]	NP	46.6	30.4	4.5	3.8	4.2	3.9	-	0.6
[101]	CCA	62.34	9.55	12.65	10.16	1.33	0.55	1.3	0.61
[24]	WGP	70.30	2.20	10.64	0.82	0.96	11.21	0.33	-
[102]	CBA	14.65	13.96	62.24	2.94	1.95	0.75	0.93	-
[67]	LKD	14.6	0.2	80.1	0.1	0.6	3.8	-	0.3
[103]	FCC	49.61	46.23	0.09	0.70	0.19	0.70	-	0.70
[104]	POFA	66.91	6.44	5.56	5.72	3.13	0.19	0.33	-
[105]	BP	57.67	14.91	9.81	5.02	3.47	1.45	1.86	-
[106]	PA	59.06	6.05	15.02	5.22	2.04	0.24	1.72	-
[107]	RAP	3.15	4.78	40.98	0.10	36.80	-	0.89	-

2.1.2. Alkaline Activators

The use of activators for activating the precursor materials plays a significant role in generating cementitious materials through the geopolymerization process. Activation allows the crystallization and precipitation of alumina and silica components of the solution. Hydroxide ions act as a reactivity catalyst while the cation of metal acts as a structural element, balancing the negative framework of the tetrahedral aluminum [108,109]. Initially, the reaction is based on the dissolution ability of the activator on pozzolanic materials as well as the production of reactive aluminum and silicon in the solution.

With the mixture of the alkaline activator and pozzolanic materials, vast dissolution of the vitreous component occurs. In this case, space and time are not adequate for the growth of the gel into a well-crystallized structure, forming semi-crystalline, amorphous, or microcrystalline structures [52].

The activating agents can be categorized into the following where M is an alkali ion: silicates, M_2O*nSiO_3, strong salt acids, M_2SO_4, aluminosilicates, M_2O*nAl_2SO_3*(2–6)SiO_2, weak acid salts, M_2CO_3, M_2SO_3, M_3PO_4, MF, aluminates, M_2O*nAlO_3, and alkalis, MOH (Pacheco-Torgal et al.). Examples of activators include K_2CO_3, KOH, NaOH, cement clinker, K_2SO_4, Na_2CO_3, and Na_2SO_3 [72,110]. The most widely used activators are NaOH, KOH, and Na_2SO_3 [111,112], which are described below.

(1) Sodium Hydroxide (NaOH)

Sodium hydroxide widely used for the production of geopolymer binders. In comparison to potassium cations, sodium cations are smaller and can move within the paste network with a relatively smaller effort, thereby providing enhanced zeolitization. It also carries a high charge density, prompting more formation of zeolite energy [108,109].

High content of the sodium hydroxide activator can depress carbon hydrogen and ettringite and accelerate chemical dissolution during the formation of binder [113]. Additionally, high amounts of the activator result in significant strength development at the early stage of reaction though, laterally, the strength is reduced due to the substantial amount of OH^- in the solution, resulting in a non-uniform and undesirable morphology of the final product [113]. The use of NaOH in geopolymers was found to provide significant crystalline properties to the binder and thereby increased the resistance to acids and sulfate [114]. In addition, it directly impacts the formation of the main C-S-H product in the geopolymerization process as it regulates the hydration activity and buffers the pH of the fluids. An inverse relationship between the amount of activator and time of the greatest hydration heat occurs and there is a linear relationship between the generation of heat and the amount of activator [52,115].

(2) Potassium Hydroxide (KOH)

The potassium ion is more basic than other activating agents, providing a significant possibility of polymer ionization in the solution. This results in a matrix with a high ability to improve the compressive strength and porosity of the geopolymer and a dense final product with highly reactive main pozzolanic materials [116]. However, the use of a potassium activator of more than 10 M decreases the strength of the geopolymer because of the substantial potassium ions and higher Si/Al leaching of KOH-based cement in comparison with sodium hydroxide activator [116,117]. NaOH provides a higher capacity to liberate alumina and silica monomers while KOH causes a higher dissolution level as a result of a higher alkalinity level [108].

(3) Sodium Silicate (Na_2SO_3)

This activator is produced by fusing sand (SiO_2) with sodium carbonate (Na_2CO_3) at a temperature of more than 1100 °C and the use of high-pressure steam to dissolve the product into a semi-viscous liquid substance known as water-glass [118]. This substance cannot be used as an activator as it does not provide adequate activation for pozzolanic reactions. Thus, it is used in combination with sodium or potassium hydroxides for improving alkalinity and strength. Mostly, in a geopolymer binder, sodium hydroxide is mixed with sodium silicate as an activator [119]. Na_2SO_3 is commercially available in various grades, though the liquid form provides higher performance than the powdered form [112,120]. It is recommended to mix an activator of 8 to 16 M with the ratio of 2 (SiO_2/Na_2O) of silicate solution for 24 h before being used for best results [52,121].

3. Raw Materials and Mix Design

As explained above, the binders of geopolymers are manufactured by the reaction between pozzolanic precursor materials and alkaline activators [42], including: (1) dissolution,

(2) rearrangement, (3) gel nucleation, and (4) solidification. A rupture of the surface bond of the binders occurs, such as CaO and Si-O-Si bonds in GGBS and Si-O-Si and Al-O-Al bonds in FA, when the precursors are in contact with the activator, generating various dissolved substances such as calcium, alumina, and silica monomers [61]. The monomers react with each other with continuous dissolution, resulting in the formation of aluminosilicate gels. With a high content of calcium in the precursor, such as slag, the final product mainly consists of C-A-S-H gel with a tobermorite-like structure [122,123], while N-A-S-H gel is the main product when a low-calcium precursor such as FA is used [122,123]. Blending high- and low-calcium precursors results in the presence of both gels [63]. Geopolymers have been widely applied for cement replacement in concrete, mortar, soil stabilization, and pavement binders. The raw materials and the mixture designs and curing regimes of the various applications are summarized in Tables 2–4.

Table 2. Raw materials and mix design of geopolymer applications in concrete and mortar.

Ref.	Type	Binder (Weight Ratio)	Activator	L/b, W/s, S/L, or W/b	Additive (Add/b)	Aggregate Type (Agg/b)	Curing Regime
[124]	Concrete	FA (0.97) + MK (0.03)	NaOH + Na_2SiO_3 (3.2, 3.3)	L/b (0.53)	PVA (1.5) type (12/39) (1600 MPa)	Silica sand (0.26, 0.3)	80 °C (2 h) + 20 °C and 70% RH (2 d, 6 d, 27 d)
[125]	Mortar	GGBS (0.1) FA (0.9)	NaOH (1) + Na_2SiO_3 (2.5)	L/b (0.4:1)	NS (0, 0.1, 0.2, 0.3, 0.4)	River sand (1:1.5)	Ambient curing (28 d)
[96]	Mortar	DWTS (0, 0.2, 0.4, 0.6, 0.8) + GGBS (1, 0.8, 0.6, 0.4, 0.2)	NaOH + Na_2SiO_3	L/b (0.67, 1, 1.5)	-	Sand (2.75)	60 °C for 24 h and 23 °C for 28 d
[97]	Concrete	FA (0.20, 0.40, 0.55) + GGBS (0.37, 0.60, 0.80) + SF (0, 0.08)	Na_2SiO_3 (anhydrous) + water-glass	W/s (0.2)	Borax (0.051) steel (2.0, 3.0, 4.0) type (13/200) (2000 MPa)	Silica sand (0.65)	90 °C (3 d) + air curing at 23 °C (1 d)
[98]	Paste	MTs (0.535) ATs/slag (0.4/0.6)	NaOH	W/s (0.4)	-	-	20 ± 1 °C and RH ≥ 90%, then demolded and cured at 1, 3, 7, and 28 d
[126]	Mortar	WCB + GGBS + FA (0.9)	H_2O	L/b (0.1), W/b (0.4)	-	Sand (2.75)	25 °C ± 2 °C and RH 50% ± 2% at 7, 28, and 90 d
[99]	Paste	SFCC + MK (0.1:0, 0.9:0.1, 0.8:0.2, 0.7:0.3, 0.6:0.4, 0.5:0.5)	Na_2SiO_3 + H_2O	S/L (0, 05, 1, 1.5, 2, 2.5, 3)	-	-	60 °C for 6 h, followed by curing at room temperature for 7 d
[127]	Concrete	FA	NaOH + Na_2SiO_3	W/b (0.32)	-	Sand, coarse aggregate	Ambient temperature for 7 and 28 d
[100]	Paste	GGBS (0.5) SSA (0.5)	NaOH + Na_2SiO_3	W/b (0.35)	-	-	Ambient temperature for 7 and 28 d
[128]	Concrete	FA	Na_2SiO_3 :NaOH (0.4, 0.45, 0.5)		SP (12 kg/m^3) NC (0, 1, 0, 1) NT (0, 0, 1.25, 1.25)	Fine (720 kg/m^3), coarse aggregate (1100 kg/m^3)	Ambient temperature for 7 and 28 d
[129]	Mortar	FA (0, 0.5) + GGBS (0.5, 1.0)	Na_2SiO_3 (anhydrous)	W/s (0.4)	PE (0–2.0) type (13/17) (3000 MPa) + steel (0–2.0) type (13/180) (2850 MPa)	Silica sand (0, 0.03)	Water curing (27 d)
[130]	Mortar	FA (0.1) + GGBS (0.9)	NaOH + Na_2SiO_3 (3.2)	L/b (0.54)	PE (2.0) type (12/24) (3000 MPa)	Silica sand (0.3)	80 °C (2 h) + 20 °C and 70% RH (0–119 d)
[101]	Concrete (two grades of strength, C 30 and 40 MPa)	GGBS CCA (0–100 wt% of GGBS by CCA)	Na_2SiO_3 + NaOH (2.5:1)	-	-	Fine (720 kg/m^3), coarse aggregate (1045 kg/m^3)	Immersed in a water curing tank for 28 d
[102]	Concrete	GGBS + CBA (1:0, 0.8:0.2, 0.6:0.4, 0.4:0.6, 0.2:0.8, 0:1)	Na_2SiO_3 + NaOH (2.5:1)		SP	River sand (681.56 kg/m^3) and granite (1034.73 kg/m^3)	Ambient curing for 7, 14, 28, 56, and 90 d
[4]	Concrete (two grades of strength, C 30 and 40 MPa)	FA (0.5), GGBS (0.32)	Na_2SiO_3 (0.09) + Na_2CO_3 (0.09)	-	WR (0, 1.91, 1.74 kg/m^3) HWR (0, 0.9, 0.77 kg/m^3)	Coarse sand fine sand	Ambient curing (28 d)
[131]	Paste	GGBS (generated by charcoal and NaOH (0.05))	Na_2SO4 (0.05) and $MgSO_4$ (0.05)	W/s (0.45)	-	-	7 d (before immersion in either Na_2SO_4 or mgso4 solution) and 49 and 91 d (after immersion in Na_2SO_4 or $mgso_4$ solution)
[67]	Paste	MK:LKD (0.5:0.5, 0.75:0.25, 0.25:0.75) MK:LKD:NP (0.25:0.65:0.1) MK:LKD:NP (0.4:0.4:0.2)	LKD, NP	-	-	-	50 °C for 7 d and then cured in normal water at 20 °C until 28 d
[132]	Concrete	FA (0.8) + GGBS (0.2)	NaOH (10) + Na_2SiO_3 (2.0)	L/b (0.4, 0.45)	SP (0.01) PVA (1.0, 1.5, 1.75, 2.0) + RTS (0, 0.25, 0.5)	Silica sand (0.1, 0.4)	20 °C and 60% or 95% RH (6 d, 27 d)
[103]	Paste	FCC	Na_2SiO_3 + NaOH (7.5 M, 10 M, 12.5 M and 15 M)	L/b (0.8 to 2.0)	-	-	1 d at 65 °C and 6 d at room temperature

Table 2. *Cont.*

Ref.	Type	Binder (Weight Ratio)	Activator	L/b, W/s, S/L, or W/b	Additive (Add/b)	Aggregate Type (Agg/b)	Curing Regime
[133]	Concrete	GGBS (0.94, 1.0) + SF (0, 0.06)	$Ca(OH)_2$ + Na_2SO_4, $Ca(OH)_2$	W/s (0.21–0.45)	SP (0.0039–0.40) + VMA (0, 0.002, 0.01) + defoamer (0, 0.001, 0.1) PVA (1.0, 1.3) PE (1.5, 1.75, 2.0)	-	Air curing at 23 °C (26 d), water curing at 23 °C (1–88 d)
[114]	Paste	GGBS FA	NaOH	L/b FA (0.3) L/b GGBS (0.4)	-	-	GGBS for 20 h in a climatic chamber (99% RH, 21 °C) and FA for 20 h in an oven at 85 °C, with RH 99%, followed by curing at room temperature for 2 d or 28 d
[104]	Concrete	POFA (1.0)	NaOH (8) + Na_2SiO_3 (3.3)	L/b (0.50–0.65)	SP (0, 0.05, 0.10)	Dune sand (1.8)	65 °C (1 d) + air curing at 25 °C (126 d)

Note: FA = fly ash, GGBS = ground granulated blast furnace slag, MK = metakaolin, NS= nanosilica, DWTS = drinking water treatment sludge, SF = silica fume, MTs = mine tailings, ATs = activated tailings, SFCC = spent fluid catalytic cracking, SSA = sewage sludge ash, NC = nanoclay, NT = nano-TiO_2, CCA = corncob ash, CBA = cow bone ash, WR = water reducer, HWR = high-range water reducer, WCB = waste clay brick, LKD = lime kiln dust, NP = nanoparticles, FCC = fluid catalytic cracking, POFA = palm oil fuel ash, SS = steel slag, SP = superplasticizer; VMA = viscosity-modifying admixture, PVA = polyvinyl alcohol, PE = polyethylene, PP = polypropylene, RTS = recycled tire steel, RH = relative humidity, M= molarity, L/b = liquid-to-binder ratio, W/s = water-to-solid ratio, S/L = solid-to-liquid ratio, W/b = water-to-binder ratio, Add/b = additive-to-binder ratio, Agg/b = aggregate-to-binder ratio, h = hours, d = days.

Table 3. Raw materials and mix design of geopolymer applications in soil stabilization.

Ref.	Soil Type	Binder (Weight Ratio)	Activator	L/b, W/s, S/L, or W/b	Curing Regime
[134]	Poorly graded clean sand (SP)	FA (partial replacement with dry soil for 5 min of 0.1, 0.15, 0.2)	NaOH + Na_2SiO_3	L/b (0.4, 0.6)	Kept for 24 h before being soaked in water for 28 d
[135]	Clay	MK (0.08, 0.1, 0.12, 0.14)	Na_2SiO_3 + NaOH (0.5:1)	S/L (0.38)	23 °C to completion for 1 d, 3 d, 7 d, 14 d, and 28 d
[136]	Lateritic soil (MLS)	MLS:BA (0.7:0.3, 0.5:0.5, 0.3:0.7)	Na_2SiO_3:NaOH (0:1, 0.1:0.9, 0.7:0.3, 0.5:0.5, 0.3:0.7, 0.8:0.2)	S/L (0.05–0.2)	At room temperature for 7 d
[137]	Bentonite soil (CH) Dispersive soil (CL-ML)	FA (0.05, 0.1, 0.15) PA	Na_2SiO_3 + NaOH (2:1)	L/b (0.1:0.4)	3, 7, and 14 d (wrapped in cling film and left at 32–35 °C and 50–60% RH)
[138]	Loess	1. MK (0, 0.025, 0.05, 0.075, 0.10, 0.2, 0.25, 0.3) 2. MK (0.3)	1. Na_2SiO_3 + NaOH 2. Na_2SiO_3 + CaO (0.01, 0.05, 0.1, 0.15, 0.2)	-	Dried for 28 d
[139]	High-plasticity clay (CH) Low-plasticity clay (CL)	MK (0.04, 0.1, 0.15)	NaOH (0.2–0.4) + KOH (0.2–0.45)	W/s (0.1–0.5)	0 (6 h), 7, and 14 d wet–dry cycle (submerged in water for 5 h, then placed in an oven at 70 °C for 48 h)
[140]	Silty clay	MK (0.06, 0.08, 0.1, 0.12)	CaO +$NaHCO_3$ (1:1)	L/b (0.03, 0.05, 0.07, 0.09, 0.11)	Curing for 1 d, 3 d, and 7 d
[141]	Black cotton soil (BC)	GGBS (0.1, 0.2, 0.3, 0.4, 0.5)	NaOH (3–12 M)		Wrapped in plastic film for curing of 28 d wet–dry cycle (submerged in water for 5 h, then placed in an oven at 71 ± 3 c for 42 h)
[106]	Marine soft clay (CL)	PA (0, 0.03, 0.06, 0.08, 0.11, 0.14)	CCR (0.06, 0.08, 0.1, 0.12, 0.14, 0.16) NaOH (0.1)	W/s (0.615)	RH ≥ 97%; 20 ± 0.5 °C for 7, 14, 28 d
[142]	Silty sand	FA and GGBS (0.1)	NaOH + Na_2SiO_3		RH ≥ 97%; 20 ± 0.5 °C for 7, 14, 28 d
[143]	Sandy clay	FA (0.2–0.4)	NaOH + Na_2SiO_3	L/b (0.4, 0.5)	At room temperature for 28 d

Note: FA = fly ash, GGBS = ground granulated blast furnace slag, MK = metakaolin, BA = bottom ash, PA = plant ash, RH = relative humidity, M= molarity, L/b = liquid-to-binder ratio, W/s = water-to-solid ratio, S/L = liquid-to-solid ratio, W/b = water-to-binder ratio, Add/b = additive-to-binder ratio, Agg/b = aggregate-to-binder ratio, h = hours, d = days.

Table 4. Raw materials and mix design of geopolymer applications in pavement.

Ref.	Binder (Weight Ratio)	Activator	L/b, W/s, or W/b	Additive (Add/b)	Aggregate Type (Agg/b)	Curing Regime
[144]	FA (0.03, 0.06, 0.09 by mass of the asphalt binder)	NaOH + Na_2SiO_3 (1:0.5)	L/b (0.)	-	-	For 24 h, 6 d, and 13 d at room temperature, then in oven at 40 °C for 24 h
[145]	GGBS- FA (0.02:0.08, 0.03:0.12, 0.04:0.16, 0.05:0.2) cement-FA (0.03:0.12, 0.04:0.14)	GGBS-based geopolymer composed of slag and alkaline activator cement	-	-	-	(20 ± 3) °C and RH > 90% for 7 d
[12]	FA:GGBS (0.4:0.6, 0.6:0.4, 0.4:0.5, 0.63:0.35, 0.45:0.45)	Na_2SiO_3:NaOH (1.5, 2, 2.5)	L/b (0.4, 0.45, 0.5)	SF (0.4)	River sand (600 kg/m^3) A nonreactive basalt aggregate (360 kg/m^3) (1:1.5:3, binder to fine and coarse aggregates)	23 ± 2 °C and RH of 50 ± 4% for air drying for 7, 56, 112 d
[146]	MK:WBP (0.85:0.15)	Na_2SiO_3:NaOH (2)	L/b (0.65)	SP (0.02, 0.1)	Natural sand (475 kg/m^3) natural crushed gravel (ca) (1240 kg/m^3) BA:CA (0.1) PL:CA (0.1) WBP:BA:CA (0.1:0.15) WBP:PL:CA (0.15:0.1)	After 24 h, the demolded samples were covered with thick nylon and kept inside an electrical oven at 50 °C for 45 h till test time
[147]	FA	Na_2SiO_3:NaOH	L/b (0.4) W/b (0.2)	-	Narmada river sand (547 kg/m^3) Crushed basalt stone (1277 kg/m^3) (1: 1.3: 3.2, binder to fine and coarse aggregates)	Thermally cured at 60 °C for 24 h, then at ambient temperature for 7, 14, 21, and 28 d
[148]	OPC (1) FA (1)	NaOH (8, 10, 12 M) Na_2SiO_3:NaOH (1.5, 2, 2.5, 3)	W/c (0.4) S/L (1.5, 2, 2.5, 3)	-	Fine aggregates (1.84) Coarse aggregates (2.65)	At room temperature for 28 d
[149]	FA (0.2, 0.15)	Na_2SiO_3:NaOH (2.5)	L/s (0.5) W/s (0.05, 0.35)	-	Crushed aggregate Coarse and fine aggregates/whole mixture by mass (0.8, 0.85)	At room temperature 7, 28, and 90 d of curing
[107]	RAP:GGBS (0.8:0.2, 0.9:0.1)	NaOH:Na_2SiO_3 (1:0, 0.7:0.3, 0.6:0.4, 0.5:0.5)	L/b (0.09–0.16)	-	-	At room temperature for 7 and 28 d

Note: FA = fly ash, GGBS = ground granulated blast furnace slag, MK = metakaolin, WBP = powder of clay brick waste, BA = recycled clay brick waste aggregate, CA = coarse aggregate, PL = plastic waste aggregate, OPC = ordinary Portland cement, RAP = recycled asphalt pavement. SP = superplasticizer, RH = relative humidity, M= molarity, L/b = liquid-to-binder ratio, W/s = water-to-solid ratio, S/L = solid-to-liquid ratio, W/b = water-to-binder ratio, Add/b = additive-to-binder ratio, Agg/b = aggregate-to-binder ratio, h = hours, d = days.

For preparing concrete, mortars, or pavement-based geopolymers, GGBS and FA have been used as 10–50% and 50–90% of the total mass of the binder. These were either blended or used with other supporting materials made of waste and by-products. MK is used as a separate pozzolanic material or blended with FA or waste by-products with a content of up to 1.5%. Apart from GGBS, FA, and MK, waste and by-product materials have also been used as precursors for producing concrete and mortar due to their environmental benefits. Several additives, including superplasticizers, nanoparticles, fibers, and silica fumes, can be used for improving the viscosity and rheology of the structure and strength of the concrete or mortar due to pozzolanic reactions. As fine aggregates, silica or river sand with a maximum particle size of less than 1180 µm has been used. While traditional coarse aggregates have been used in some applications (i.e., mortars and pastes), their use is limited as they can increase the fracture toughness of the matrix and impair tensile characteristics [64]. For reducing the environmental impact of using natural resources, crushed recycled granite, basalt, and copper have been used as a replacement for fine or coarse aggregates. The ratio of aggregate to binder ranged from 0.2 to 5.

For soil stabilization, most of the geopolymer studies utilize MK and traditional precursors of FA and GGSB. MK content was up to 50% of the total mass of the binder while FA and GGSB contents were up to 20% and 50% of the total mass of the binder, respectively. Bottom ash and plant ash could be used as possible alternative precursors.

Generally, a combination of sodium hydroxide (NaOH) and sodium silicate (Na_2SiO_3) was the most used liquid alkaline activator for geopolymer precursors. The molarity of NaOH ranged from 4 to 20 M while the modules of silicate (SiO_2/Na_2O) of Na_2SiO_3 ranged from 2 to 3. A large amount of heat is released by blending these solutions which requires the use of a cooling system before usage. Other solid activators such as Na_2SiO_3 have been explored as a solid alternative activator. The liquid-to-binder ratio ranged from 0.1 to 0.8 and the water-to-solid ratio from 0.2 to 0.5.

4. Results and Discussion

4.1. Concrete and Mortar

It is reported that only 3% of the studied mixtures provided 10 to 40 MPa of compressive strength, which can only be applied to some non-structural applications [150], whereas 40% of researchers reported compressive strength higher than 40 MPa, adequate for structural applications. The increase in the curing period up to 28 days significantly increased the compressive strength of geopolymer, then it slightly increased or reduced [124,130]. The reduction can be attributed to the induced cracking from shrinkage. The highest reported compressive strength is 222 MPa, though with a low strain capacity of less than 0.4% [97]. The binding of GGBS and FA provided 100 MPa as the highest compressive strength with a 5.77 MPa tensile strength and a 5.81% tensile strain capacity [130].

The tensile stress–strain behavior of geopolymer concrete and mortars can be divided into three areas, namely linear elastic, strain softening, and strain hardening areas. Between strain hardening and linear elastic areas, the transition point is known as the first cracking strength [129]. The tensile strength represents the highest stress point with corresponding strain being the capacity of tensile strain. Additionally, the strain hardening can be reflected by the density of strain energy per unit volume, obtained by the integration of the tensile curve of stress–strain before the area of strain softening [151]. Few studies reported a pure strain softening response while most studies reported a clear strain hardening response [7].

Workability is a significant characteristic of geopolymer concrete, usually evaluated using a flow table test [7]. The specimens prepared from GGBS have lower slump flow than the FA–GGBS-based geopolymer binders due to the low reactivity and spherical shape of FA [151]. The increase in the amount of activator reduces the slump flow value [7], due to polycondensation and accelerated dissolution. However, [104] reported an opposite trend due to the different precursors used. In addition, the increase in the W/s or W/b ratios results in increasing the workability of concrete [133], while the slump flow was consistently reduced with the increase in Agg/b ratio as a result of the larger specific area and interparticle friction [132]. More paste is required with a large specific area for converting the aggregates while the packing of particles can be improved with a high content of aggregates which requires less paste for filling the voids [152]. Such factors simultaneously compete and the use of a proper content of aggregates can result in a better packing of particles and adequate workability of concrete.

Eliminating the use of coarse aggregates results in higher dry shrinkage during the hardening process [153]. Paste geopolymer binders are more susceptible to dry shrinkage and cracking in comparison with geopolymer concrete. The use of a high content of coarse aggregates in geopolymer concrete provides more resistance to drying shrinkage [132]. Controlling drying shrinkage is investigated in only limited studies.

The durability of FA–GGBS and FA-based geopolymer concrete was only studied in a few studies, therefore further research is needed on the impact of other attack types such as carbonation. Different kinds of sulfate solution provide variable impacts on the alkali-activated slag geopolymers. Immersion in Na_2SO_4 did not impact or cause any harmful consequences on the binder other than positively impacting on further activation of the slag. On the other hand, the use of $MgSO_4$ aggressively impacts the geopolymer, leading to the decomposition of hydration products and the formation of gypsum. Such an attack is associated with disintegration rather than expansion. Accelerating the sulfate attack with the use of a small amount of paste is an efficient technique. Additionally, the expansion can be reduced by wrapping the specimens [131].

The study by Ruiz et al. [103] indicated that the SiO_2/Al_2O_3, Na_2O/SiO_2, Na_2O/Al_2O_3, and H_2O/total solids ratios in both precursor and activator can be controlled for the best performance of geopolymers. Ruiz et al. [103] found the compressive strength reached the highest level at 7 days of curing with the use of a 1.10 concentration of AS/FCC, 15 M of NaOH, and 0.85 Ms modulus. In comparison with other geopolymer binders, the density was lower.

Table 5 summarizes several studies carried out on the synthesis and performance of geopolymers from several low-reactivity precursors with their resulting compressive strengths. High curing temperatures and supplementary active materials can promote geopolymerization and increase the compressive strength of low-reactivity geopolymer binders. However, in actual engineering applications, achieving high curing temperatures is relatively difficult. A pretreatment of 550–1100 °C followed by ambient curing was performed on precursors for alkaline fusion with the addition of supplementary cementitious materials for enhancing performance. In addition, the associated cost of high-temperature requirements for calcination during the fusion process has substantially reduced the practical application of this technique. The compressive strength of most geopolymer binders reaches above 35 MPa after 28 days of curing at ambient temperature, which shows the great possibility of application in construction.

Table 5. Summary of geopolymers from several low-reactivity precursors with their compressive strengths.

Ref.	Inert Precursors	Pretreatment Method	Supplementary Materials	Alkaline Activator	Curing Temperature	Compressive Strength
[154]	Red mud	Alkali fusion at 800 °C for 1 h	25 wt% of silica fume	-	Ambient temperature	28 d: ~31.5 MPa
[155]	Bentonite	Alkali fusion at 1100 °C for 3 h	-	-	80 °C for 72 h, ambient temperature	28 d: ~38.3 MPa
[156]	Phosphate tailings	-	50 wt% of metakaolin	NaOH	80 °C for 24 h, ambient temperature	14 d: ~53.0 MPa
[157]	Vanadium tailings	Mechanical activation	50 wt% of metakaolin	Na_2SiO_3	Ambient temperature	14 d: ~25.0 MPa
[158]	Copper tailings	-	10 wt% of fly ash	Na_2SiO_3 +NaOH	80 °C for 48 h, ambient temperature	28 d: ~36.9 MPa
[159]	Granite waste	Alkali fusion at 550 °C for 2 h	40 wt% of metakaolin	Na_2SiO_3	Ambient temperature	28 d: ~40.5 MPa
[160]	Volcanic ash	Alkali fusion at 550 °C for 1 h	30 wt% of metakaolin	Na_2SiO_3	Ambient temperature	28 d: ~41.5 MPa

Liu et al. [98] used only 200 °C for the hydrothermal process for activating MTs, indicating reduced costs of geopolymers in comparison with the conventional fusion technique. The resulting strength was about 48 MPa at 28 days of ambient curing, which could be applied in general construction fields. As shown in Figure 7, the compressive strength of geopolymer binders was higher than that of normal concrete, indicating that a hydrothermal process is an effective approach for improving the reactivity of MTs. With the increase in the NaOH content to 30%, the compressive strength increased for geopolymer concrete samples. For slag hydration, an alkaline environment was produced during the hydrothermal process that generated soluble products from the reaction of activators with precursors. This phenomenon was also described in other slag-based cementitious materials containing high alkali content [161,162].

The content of C(N)–S–H gel as a dominant reactant is impacted by the content of the activator. Increasing NaOH enhanced the initial pH, dissolving alumina and silica species from precursors and thereby increasing the amount of produced gel (Figure 8a,b). This occurs up to a certain level of activator with any further increase in the activator content beyond this level negatively impacting the microstructure. This is shown in Figure 8c by the presence of microcracks and micropores due to the excessive amount of free alkali [98].

Thermal treatment was investigated at two temperatures of 950 °C and 450 °C for increasing the reactivity of geopolymer binders when lime waste (LKD) material was used as an activator [67]. It was evident that the thermal treatment was contributing to the breakage of crystalline phases of the material by transforming it into an amorphous structure, particularly at 450 °C, indicated by XRD, TG-DTA, and FTIR results. Kadhim et al. [67] reported the possibility of using lime waste as an activator if adequately treated and impurities are removed.

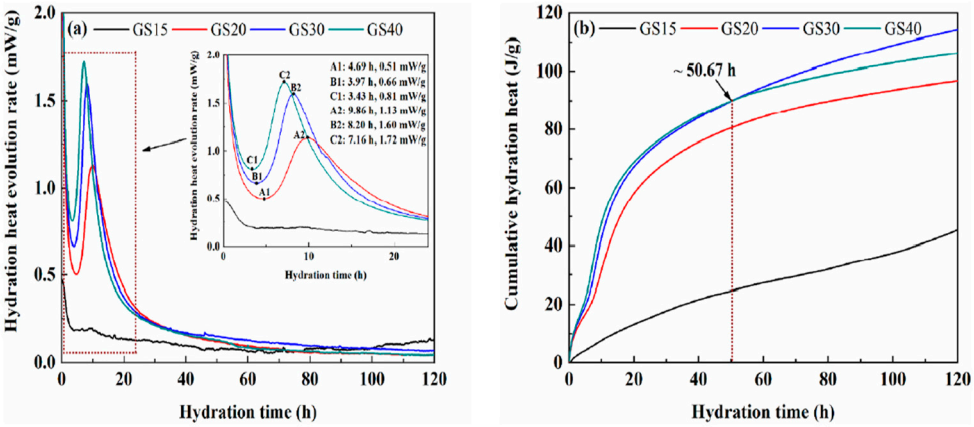

Figure 7. Impact of activator on hydration heat rate and cumulative hydration heat [98]. (**a**) heat hydration flow curves (the acceleration period and deceleration period), (**b**) cumulative heat curves of geopolymer binders with different NaOH contents.

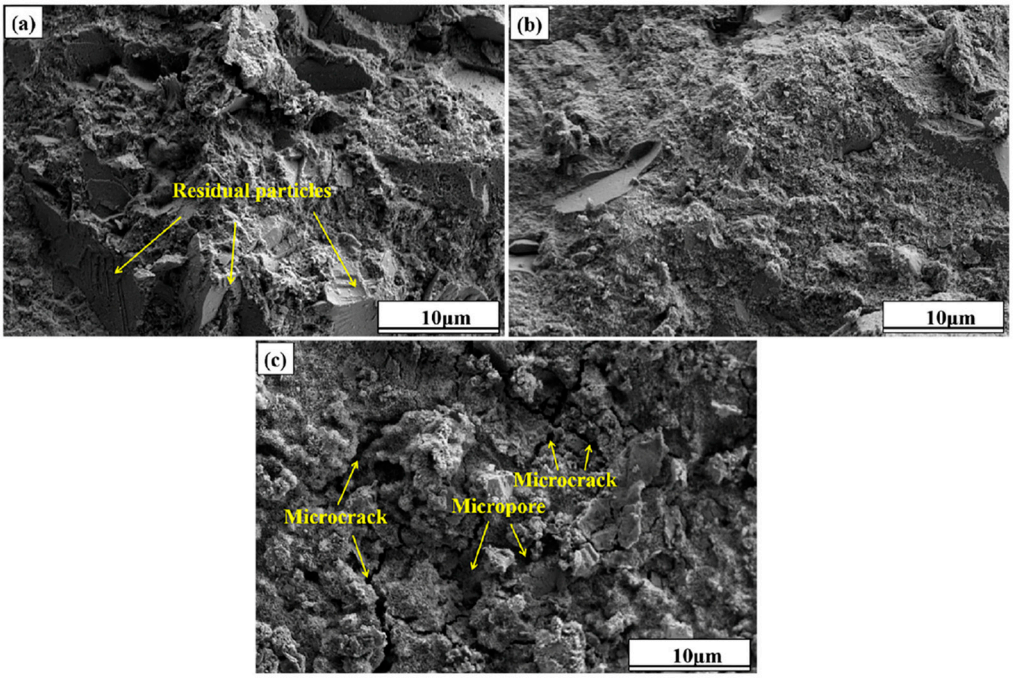

Figure 8. Impact of activator on the microstructure of MT geopolymer concrete [98].

Garcia Lodeiro et al. [114] reported that aluminum extrusion by-products can effectively be used as an activator for low-alkalinity precursors such as calcium and silicon high blast furnace slag binder. This provides similar mechanical and hydration properties to conventional 4M-NaOHBFS paste. However, the activator is not sufficient for dissolving all alumina and silica specimens in high-reactivity systems such as FA-based geopolymers, as shown by low mechanical and hydration properties.

As per various design specifications shown in Figure 9, Akhtar et al. [127] reported that normal cement concrete provides compressive strengths of 41 MPa, 43 MPa, and 32 MPa at 28 days of curing per IS, ACI, and DOE specifications, respectively. These were compared with FA-based geopolymer concrete. They concluded several points: (1) geopolymer is a cement-free binder, (2) design methods by the IS standard provided a higher estimation of cement requirements, (3) the highest compressive strength was obtained for geopolymer binder with NaOH+Na_2SiO_3 as an activator of about 48 MPa at 28 days at an initial 80 °C for 24 h of curing; 80% of gain strength was even obtained at 7 days of curing, and (4) the

slump value was the lowest for the geopolymer concrete while mixtures according to the IS standard had the highest slump levels.

The compressive strength of FA-based geopolymer concrete was enhanced with the use of nanoparticles (NC, TiO_2) by 38% for NC and 24% for TiO_2 for binary binders [128]. Additionally, nanoparticles were proved to be significant elements in enhancing the tensile strength of geopolymers with a higher strength as a result of the use of NC in comparison with NT. The use of nanomaterial at more than 1% lowered the obtained improvements [128]. It is suggested that, for better utilization, the amount of nanomaterials is limited to 1%.

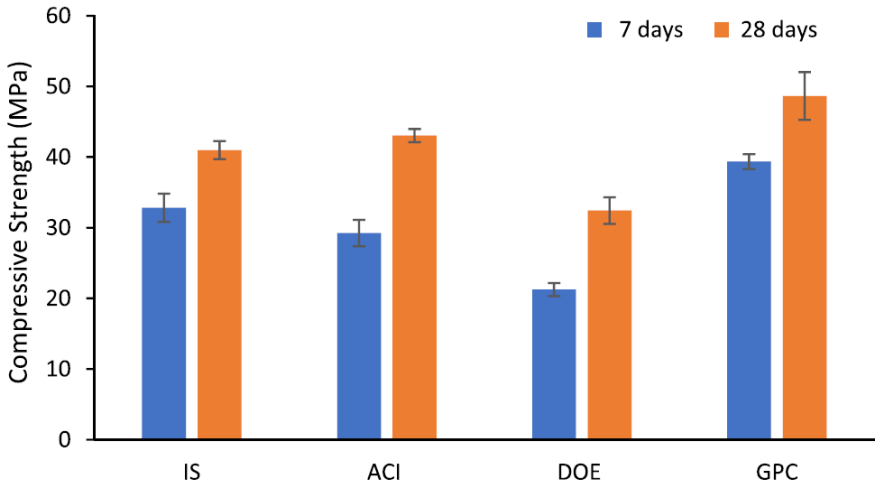

Figure 9. Compressive strength of normal concrete per various design specifications and FA geopolymer concrete [127].

Investigations were performed on geopolymer mortar with GGBS and FA binder and free cement with the inclusion of nanosilica [125]. The results indicated that the inclusion of nanosilica reduces the workability of mortars, showing low flow levels. The use of 1%, 2%, 3%, and 4% nanosilica reduces the flow by about 4.1%, 8.4%, 14.4%, and 21.3%, respectively. Compressive and flexural strengths improved by 30% and 33%, respectively, with the use of 1% nanosilica. The values of absorption for geopolymer mortars, as indicated in Figure 10, are in the range of 7.9% to 11.89%. The lowest water absorption was obtained for 1% NS.

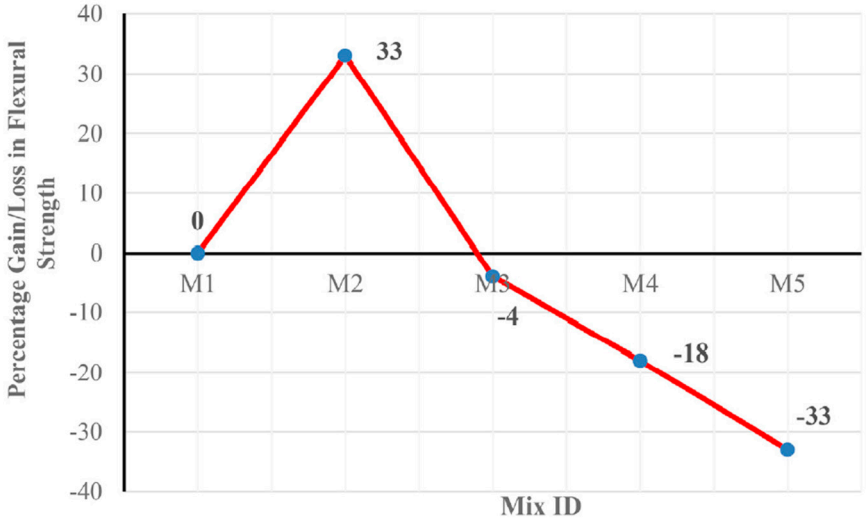

Figure 10. Gain or loss in flexural strength of GGBS-FA geopolymer mortar with the inclusion of nanosilica [125].

The use of DWTS with GGBS binder for manufacturing environmentally friendly geopolymer binder was investigated by Duan et al. [96]. The consistency of fresh mortar was significantly reduced by the reduction in the sodium silicate to sodium hydroxide ratio with the increase in the DWTS to GGBS content. This was due to the high viscosity of sodium silicate and water absorption and porosity of DWTS. The mechanical performance of GGBS-based geopolymers could be enhanced by the use of DWTS of up to 40% and a sodium silicate to sodium hydroxide ratio up to 1.5. An adequate amount of alumina is dissolved from the DWTS, promoting geopolymerization and the formation of C-A-S-H gel and providing enhanced mechanical properties. However, silica dissolution may be hindered by excessive amounts of alumina, leading to a porous matrix. This impact could be reduced with an increased sodium silicate to sodium hydroxide ratio due to extra silica provided by the activator.

The use of WGB was explored by Jiang et al. [24] who reported the significant impact of the sample sizes, as increasing the sample size reduced the compressive strength of the geopolymer paste. Smaller samples can result in higher reaction degrees as well as higher relative humidity and curing temperature. These contribute to the formation of the C–S-Hs and lead to better mechanical performance. Additionally, the XRD, TGA/DSC, mass loss, and carbonation test results indicated the significant impact of moisture distribution, causing different impacts during the geopolymerization process at different reaction stages.

WCB was investigated in GGBS–FA-based geopolymer mortars by Migunthanna et al. [126] as an alternative to normal cement-based geopolymer mortars. WCB did not result in mechanical property improvements. Immersing the mortars in water reduced the strength by up to 27% after 1 month, while some samples were not impacted by the immersion. Most samples had good performance even with water susceptibility. Enhanced resistance to sulfate attack with a maximum expansion of 0.12% was reported by the use of WCB-based geopolymers in comparison with normal cement mortar. In addition, exposing WCB-based geopolymers to sulfate for up to 150 days did not noticeably impact the compressive strength, dimensional stability, or microstructure. WCB-based binders can be used to replace OPC in mortar for developing low-carbon and high-performance material.

Rovnaník et al. [105], on the other hand, investigated BP and fly ash-based geopolymers with a ratio of 1:3. The results, as shown in Figure 11, indicate compressive strengths of 40 MPa and 48 MPa at 28 and 90 days of curing, respectively. The use of a ratio of 1:1 did not provide significant changes in the compressive strengths across the curing periods. Similarly, Wong et al. [163] explored the combination of WCB and fly ash in 10 and 20% replacements for preparing geopolymer mortars. They reported a compressive strength of 44.2 MPa at 28 days from the replacement of fly ash by 10% WCB. There are no significant differences in the reported compressive strength in either study with 10% and 50% replacements of fly ash with WCB. Migunthanna et al. [126] reported a similar relationship when preparing geopolymers from WCB and fly ash, which indicated a non-significant improvement of compressive strength beyond the 40% replacement of fly ash.

SFCC catalyst contains nickel in the stable forms of $NiSiO_3$ and $NiAl_2O_4$ [99]. This nickel is partially dissolved when the SFCC catalyst is used for preparing a geopolymer concrete binder with tetrahedral aluminum of negative charge in the geopolymers. On the SFCC catalyst, the faujasite absorbs the main form of vanadium in the catalyst. The faujasite zeolite structure during the alkali excitation process dissolves, leading to the dissolution of adsorbed vanadium. During this process, the vanadium oxide reacts and is converted to vanadate with a negative charge and the ability to dissolve in water. Thus, physical encapsulation or charge balance cannot immobilize the vanadium in the catalyst. However, the vanadium can effectively be removed by pretreatment with oxalic acid without impacting the nickel stability in the geopolymers, leading to non-metal leaching geopolymers [99]. Similarly, Zhang et al. [164] found that the replacement of MK with SFCC catalyst in an appropriate amount can improve the compressive strength of geopolymers according to the quadratic model. However, the compressive strength was reduced by the use of a significant amount of SFCC catalyst. A 20% replacement provided the highest

compressive strength which was two times that of MK-based geopolymer binder. The highest compressive strength of 41.22 MPa was obtained with the 20% replacement of SFCC catalysts, which was 21.6% higher than that of the geopolymers without SFCC catalyst. The microstructure and crystal structure analysis indicated that the SFCC catalyst partially participated in the geopolymerization.

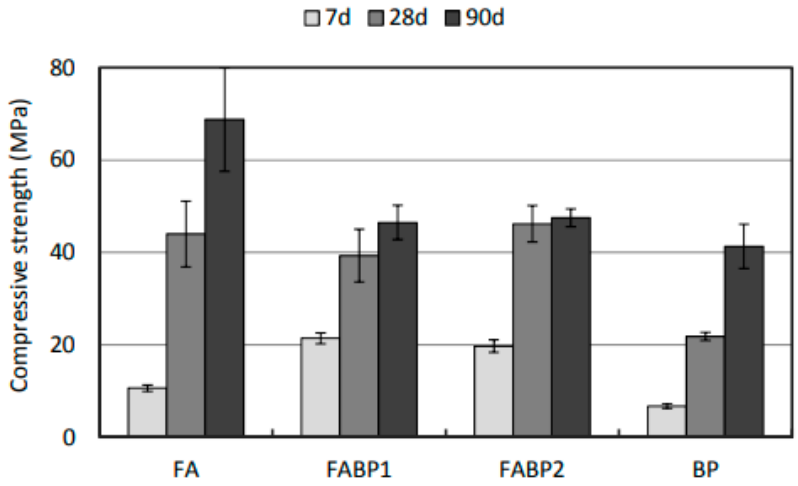

Figure 11. Compressive strengths of prepared geopolymer paste at the ages of 7, 28, and 90 days [105].

The use of SSA with GGBS as precursors with various contents of Na_2O as an activator was explored by Zhao et al. [100]. The Na_2O content or the modulus of the activators initially increased and then decreased the compressive strength of the geopolymers. The highest compressive strength was obtained at a Na_2O content of 6% and 1.2 modulus of the activator. The presence of crystals and quartz in the SSA contributes to the geopolymerization process, leading to a more amorphous structure. Heavy metals in the SSA were adequately solidified following geopolymerization with minimal leaching of the metals.

In comparison with cementitious materials, alkali-activated materials show better durability properties, being more resistant to chlorides and sulfates [165,166], acid attack [167], fire and flames [168], and water and freezing actions [169,170]. Alkali-activated materials undergo degradation from the changes in the materials' composition by exposure to aggressive environments, and the paste dissolves and becomes damaged [171].

Yang et al. [172] studied the durability of FA geopolymer paste by immersing it in 3% NaCl solutions for 72 h. They obtained satisfactory results with the combining of GGBS in the geopolymer since it acts as a filler, reducing the susceptibility to chloride ion intrusion. The use of 50% GGBS provided a denser structure and greater durability than cement-based geopolymers. Similarly, Gunasekara et al. [173] reported that the penetration of the chloride ions depends on the porosity of the matrix while reactivity depends on the content of lime, silica, and alumina as well as the surface area. A larger surface area and greater content of silica and alumina increase the formation of aluminosilicate gel and result in a less porous matrix, thereby reducing the penetration of chlorides.

The authors of some research explored the exposure to salt spray with controlled chloride concentration, humidity, and temperature [174,175], or immersion in 3.5 to 5% of NaCl solution [49,176]. Finally, most authors evaluated the effects of chloride attack through a saturation procedure in a NaCl solution followed by a drying step.

The impact of temperature is explored by Duan et al. [177] who used FA–MK-based geopolymers cured by microwave radiation. They reported a reduction in the compressive strength with the use of 300 and 400 °C due to the decomposition of the paste, leading to the dragging of Arcand water and breaking of the inner walls of the pores. However, in comparison with concrete, the performance of geopolymer was superior due to its lower mass and strength loss. In addition, Marvila et al. [178] investigated the performance of MK-based geopolymer binders at high temperatures. They found stable mechanical

properties even after firing the materials to up to 1050 °C due to the formation of zeolite. Similar results were obtained by Choi and Park [179].

Freeze and thaw resistance was studied by Zhao et al. [170] in FA–GGBS-based geopolymer binders. The study revealed that the use of 10% GGBS resulted in damaged binders after only five freeze–thaw cycles while 30% GGBS caused damage after fifty freeze–thaw cycles. The use of 50% GGBS provided the highest resistance of 225 freeze–thaw cycles, which is comparable to the freeze–thaw strength of Portland cement concrete, as shown in Figure 12. This was attributed to the denser structure by the high content of GGBS and thus more resistance to freeze and thaw. A question arises on the procedure of the durability test as there is no consensus on the experimental procedure used by authors. However, many researchers carry out the test by using a saturation cycle in chloride or distilled water for 24–48 h at ambient temperature, then a freezing period from 12 to 48 h [180–182]. The authors concluded more resistance than in cementitious compositions. Thus, although there is a certain amount of work in the literature, the results show considerable fluctuations with a range of possible causes, such as the type and amount of activators and precursors and the way to carry out the tests.

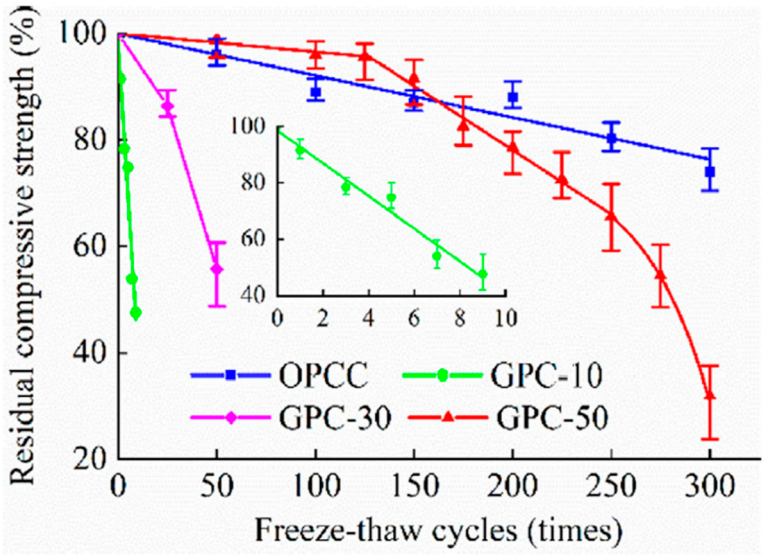

Figure 12. Residual compressive strength of concrete specimens after freeze–thaw cycles [170].

4.2. Soil

The experimental engineering program performed by Noolu et al. [141] showed that the use of GGBS-based geopolymers significantly changed the Atterberg limits and compaction parameters of treated black cotton soil (Figure 13). Compared to untreated soil, 40% GGBS with 8M of NaOH provided the highest strength by more than five times. The wetting and drying of the soil by up to 12 cycles reduced the strength by about 9%.

In a separate study, Canakci et al. [183] used various pozzolanic materials for geopolymer binders including GGBS for deep mixing improvements. The treated clay soils showed improved unconfined compressive strengths with the increase in the binder content and with the increase in the ratio of alkali liquid to GGBS of up to 1.05. Meanwhile, the experimental study by Mozumder and Laskar [184] compared the performance of GGBS and PFA geopolymer binders for the treatment of clay soil. The results showed superior performance of GGBS-based geopolymers compared to PFA-based geopolymers. Similarly, the increase in the content of the binder increased the strength of the clay due to the higher formation of cementitious gel which filled up the void spaces and increased interparticle bonds.

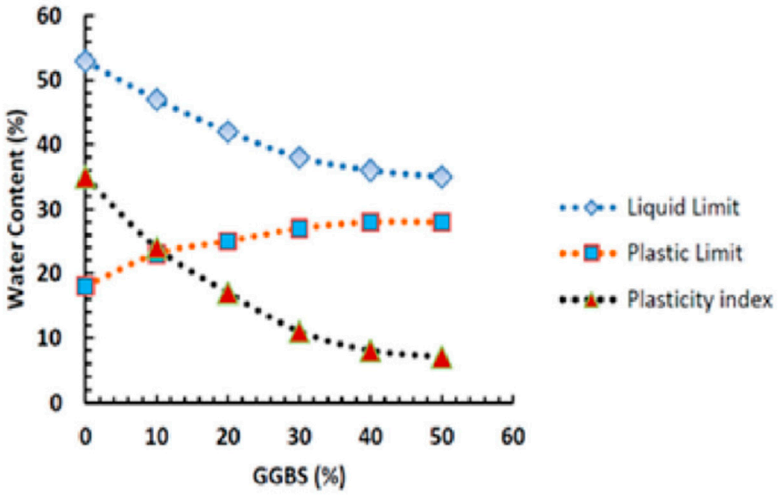

Figure 13. Variation of Atterberg limits with the addition of % GGBS [141].

The efficiency of FA-based geopolymer binder to stabilize sandy soil was investigated by Al-Rkaby et al. [134]. The results indicated brittle yielding of stress–strain curves followed by peak stress and then a sudden failure. Such behavior became stiffer with high unconfined compressive strength and low axial strain with the increase in the geopolymer binder content. In addition, the geopolymer-stabilized soil mixtures exhibited higher strengths than soil mixtures treated with normal cement due to combined pozzolanic and geopolymerization reactions. The compressive strength improvement was aligned with tensile strength improvement which was in the range of 0.4–1.2 MPa, significantly higher than that of cement-stabilized soil. The soil structure was progressively improved by the use of geopolymer stabilizers, leading to gel formation and producing an increase in strength. Similarly, Rios et al. [185] evaluated the use of FA-based geopolymers to stabilize silty sandy soil. The findings of stiffness and strength tests revealed significant improvements in the long term after 28 days of curing. However, reasonable improvements were obtained over the short term.

The use of MK-based geopolymer binders in soil in comparison with concrete requires ambient curing for practical applications. In the study by Zhang et al. [186], MK-based geopolymer was used for stabilizing weak clay. In comparison with other studies, the increase in the binder-to-soil ratio increased the compressive strength of the treated soil due to increased bonding from the effects of geopolymerization. However, the use of less than 15% geopolymer binder resulted in lower short-term strength in comparison with 5% cement by the weight of the soil. However, the long-term strength of geopolymer-treated samples was higher than that of cement-treated samples.

Similarly, the impact of curing and MK content is shown in Figure 14 [135]. The increase in the amount of MK and curing ages significantly improved the unconfined compressive strength of soft soil. Curing time and temperature are the main factors impacting the rate of strength improvement with 40 °C considered a high curing temperature compared 30 °C or 20 °C. The clay particles are covered by the hydration products. The highest compressive strength resulted from the use of MK at 10% and 12%, providing 9.9 MPa and 9.18 MPa at 14 and 7 days of curing.

The use of MK-based geopolymers for controlling dust and as a soil stabilizer of loess soil showed minimal emission of dust in comparison with traditional products such as bitumen and brine [138]. The most effective geopolymer constituents consist of 30% MK activated by sodium silicate and sodium hydroxide, providing 23.9 kN soil strength after 28 curing days [138].

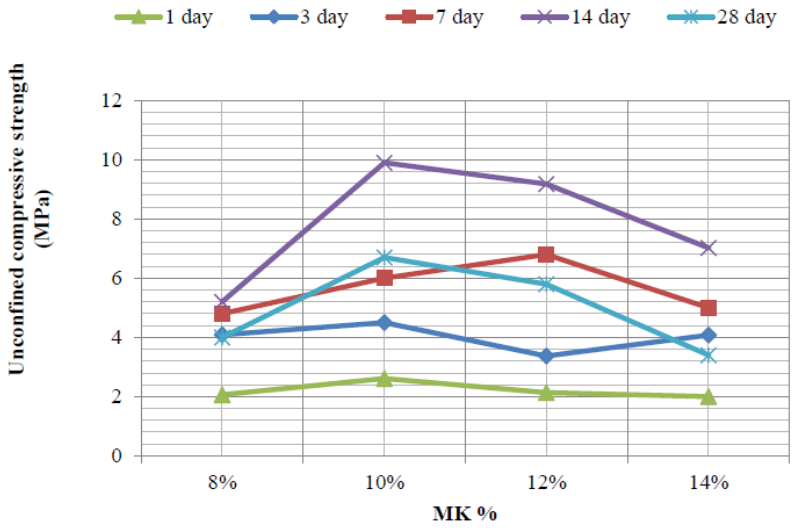

Figure 14. Impact of curing and MK content on the UCS of stabilized soil [135].

Figure 15 indicates the impact of different contents of alkaline activator (AA) and MK in binders on the UCS of treated soil [140]. It shows a maximum strength at 7 days by 5% AA and 10% MK, with about 419 kPa as a mean value, then a decrease in strength afterwards. This could be attributed to the limited amounts of calcium and sodium aluminosilicate gels when the amount of AA is more than the MK polymerization requirements, with $Ca(OH)_2$ harming the interior structure of the binder by cracking or shrinkage which results in unimproved strength over time. However, when the content of MK is significant, the hydration of lime creates weak alkalinity while Na_2SiO_3 and $Ca(OH)_2$ reactions result in a poor geopolymerization process. Thus, there should be an optimum amount of both AA and MK for maximum performance. From Figure 15, it is noted that the best content of MK and AA should be 1:2, as the geopolymer binders with the same content of MK always reach the maximum with double the AA content compared to MK. The relation between the strength and the content of GB is illustrated in Figure 15. It shows that the strength increases up to a certain level of GB and then slightly decreases. The maximum strength occurred at 15% GB. This could be attributed to the ratio of CaO and Na_2CO_3 activators of 1:1, which provides higher lime content than required for the reaction of activators in water. The amount of lime proportionately increases with the increase in the GB content, producing a high amount of $Ca(OH)_2$ and leading to cracks and shrinkage of the soil [23]. Thus, the optimum content of GB should be 15%, while economically it would be adequate to select 12% as it shows a minor difference in strength from 15% GB.

The increase in the Na_2SiO_3:NaOH ratio increased the unconfined compressive strength of soil stabilized with bottom ash geopolymers [136]. This is due to the reaction of silica and alumina from the ash with the silica from $Na2SiO_3$, leading to C-S-H and C-A-H gels. The maximum strength occurred at Na_2SiO_3:NaOH ratios of 80/20 and MLS/BA ratios of 70/30, providing 2672 kPa UCS at 7 days of curing [136].

The feasibility of using CCR to activate plant ash geopolymers and stabilize clay soil was investigated by Du and Yang [106]. The high content of activator and precursor as well as curing time increased the strength of treated soil, with maximum performance occurring at 13% plant ash, 16% CCR, and 0.8% NaOH. Brittle strength performance resulted in 1.5% to 3.5% failure strains for various contents of CCR and plant ash. The use of geopolymers increased the liquid and plastic limits and reduced the plasticity of treated soil. The development of strength can be attributed to the flocculation and agglomeration of soil particles with the dissolving of silica and alumina species as well as the production of hydration gels, leading to a dense structure.

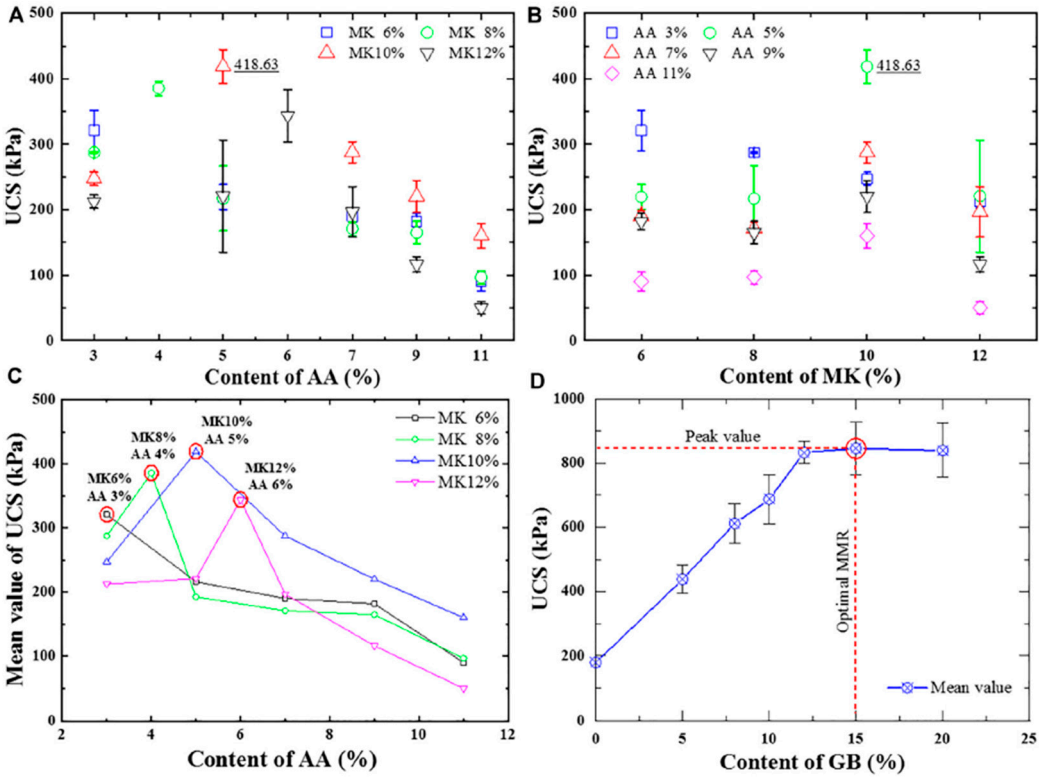

Figure 15. Impact of different contents AA, MK, and GB binders on the UCS of treated soil [140]. (**A**,**B**) display the UCS of GSC specimens with various AA and MK contents. (**C**) demonstrates the average UCS of GSC samples with various AA and MK concentrations. (**D**) shows the UCS of GSC specimens with various GB contents.

Studies on the impact of geopolymer binder on the durability of treated soil are limited and only focus on wetting–drying tests. Rios et al. [185] revealed a stable performance and reasonable residual strength by treating sand with FA-based geopolymers in comparison with cement. In terms of clay soils, Sargent et al. [142] similarly found low volumetric changes with low residual strength and attributed the low performance to the low content of clay in the soil required for cation exchange and chemical reactions. Regarding freeze–thaw resistance, only one study was found, by Abdullah et al. [187], who reported high volumetric changes and low residual strength for kaolin clay treated by FA-based geopolymers. The results suggest less unstable perforation of the soil in freeze conditions than in tropical conditions, indicating the retardation of the geopolymerization reaction at very low temperatures. On the other hand, Odeh and Al-Rkaby [188] used coal-fired fly ash geopolymers to study the mechanical and durability performance of treated clayey sandy soil. A high strength of 1–8 MPa was reported in comparison with only 0.3 MPa for untreated soils. The addition of sand to the clay reduced the optimum ratio of alkaline activator from 0.8 for clayey soil with 5% sand to 0.6 for clayey soil with 10, 20, and 30% sand. More resistance to chloride and acidic environments was reported with the use of geopolymers due to the clay fabric modification caused by interparticle contacts and the resulting bonding caused by gel formation and hardening. Swain [137] indicated reduced swelling pressure by more than 95% with the use of 15% bentonite soil and 40% FA-based geopolymers. The dispersion of bentonite was controlled by the use of an FA geopolymer stabilizer. In addition, xanthan gum and guar gum in different contents mixed with pond ash and soil provided a more durable mixture than bottom ash and soil.

It was revealed that density is inversely related to porosity, though high-density mixtures do not always ensure high strength [189]. In geopolymers, the best density which provides maximum strength is about 1.5 g/cm^3 [190]. Generally, the performance of K-based geopolymer is substantially lower than that of Na-based geopolymer, as it provides

lower shrinkage and higher strength. The increase in the content of the geopolymer binder increases the compressive strength by 90–400% for high-plasticity clay and by 150–350% for low-plasticity clay at 7 and 28 curing days [139]. High-plasticity soil soaks up more water than low-plasticity soil, and with the use of geopolymers, the water intake of high-plasticity soil is substantially reduced compared with low-plasticity soil. Mass change is reduced significantly by 10% and 4% geopolymer binders for high- and low-plasticity soils, respectively [139].

4.3. Pavement

The geopolymer concept has not been widely explored for enhancing the rheological properties of asphalt mixtures. The use of geopolymers in pavement as an alternative to asphalt modification techniques can be a more sustainable and greener approach due to its effective recycling of by-products and waste as well as lower CO_2 emission.

The results of Negahban [12] indicate the effectiveness of using FA–GGBS-based geopolymer cured at ambient temperature in in situ castings and pavement applications when compared to normal cement concrete. The use of a 0.6:0.4 ratio of FA: GGBS by weight activated by anhydrous sodium metasilicate is beneficial as it improves the pore structure, creep, shrinkage, and surface cracking. A layer-based distribution and gradation are displayed in the pore structure of geopolymer where the volume of the pores is reduced from the top to the bottom layers of the concrete section. With this, and with a subsequent profile of shrinkage, significant shrinkage reduction resulted in the restriction of the geopolymer concrete. The restrained shrinkage was reduced by 38–57% after one year, with a significant reduction in creep. This shows the lower tendencies of the geopolymer concrete surface to crack compared to normal cement concrete. With the blend of 0.6:0.4 of FA: GGBS by weight, no surface cracking was observed on the casted geopolymer concrete slab.

Experimental work on the impact of geopolymer on the properties of asphalt was carried out by Hamid et al. [144]. Noticeable impacts on the rheological properties of asphalt were reported with improved susceptibility to temperature, shear modulus, and rutting factor by the use of 3, 6, and 9% geopolymer binder. The strength ultimately increased at 7 days of curing. Figure 16 shows the relation between the failure temperature with the content of the geopolymer and the curing time of the geopolymer. Failure temperature increased with 3, 6, and 9% geopolymer, and increased to 14.2 and 15.2% with the increase in curing time to 7 and 14 days, respectively. This indicates the possibility of geopolymer enhancing the high-temperature grading of asphalt binders.

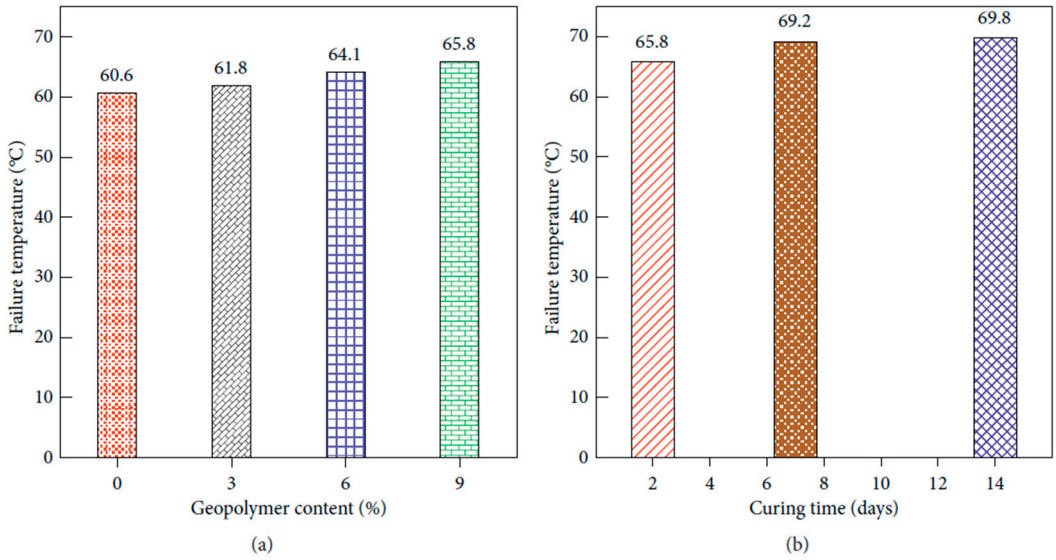

Figure 16. Impact of geopolymer content and curing time on performance grading [144]. (**a**) geopolymer content, (**b**) curing time.

Figures 17–19 indicate the effects of the content of slag geopolymer and curing times on the mechanical and durability properties of a geopolymer-stabilized macadam highway [145]. The unconfined compressive strength of the macadam stabilized by GGBS–FA geopolymer increased to 8.76 MPa and 15.4 MPa, after 7 and 28 days of curing, when a ratio of GGBS: FA: macadam of 4:16:80 was used. A linear relationship can be observed through fitting data for compressive and tensile strengths and elastic modulus with the increase in the geopolymer content. The comparison between the cement–FA-based geopolymer and GGBS–FA-based geopolymer in terms of freeze–thaw resistance and dry shrinkage shows a better performance of GGBS–FA geopolymer. The increase in the content of geopolymer from 2 to 5% decreases the loss of strength after freeze and thaw from 14.2 to 2.5%. Additionally, the strain of dry shrinkage on the GGBS–FA geopolymer content of 3% was 231.2 με in comparison with 261.3 με of FA–cement geopolymer. The cementitious materials of the geopolymer itself react, producing a stable product with high strength. The use of FA consumes a large amount of the produced $Ca(OH)_2$, improving the polymerization reaction.

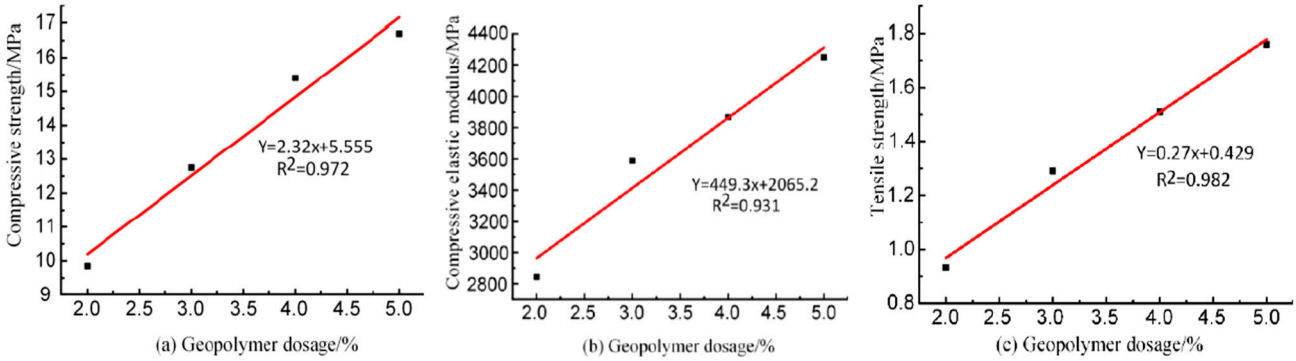

Figure 17. Effect of the content of geopolymer on the mechanical properties of geopolymer-stabilized macadam highway [145].

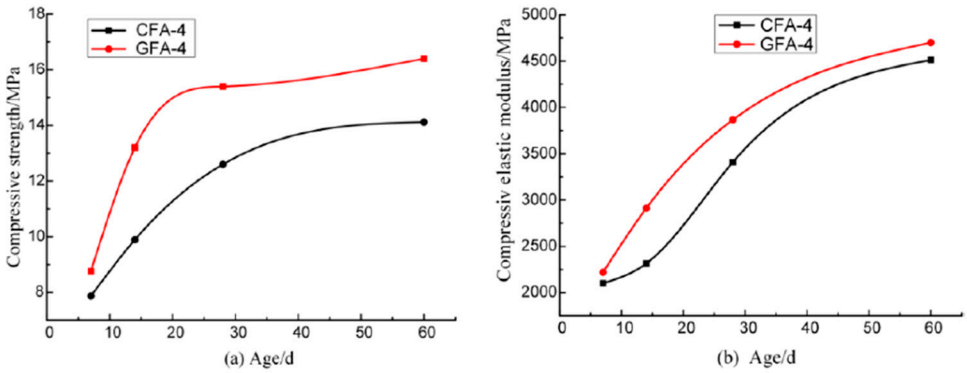

Figure 18. Effect of curing times on the mechanical properties of geopolymer-stabilized macadam highway [145].

The optimum ratio of sodium silicate to sodium hydroxide for activating the FA in pavement applications was reported to be 2.0 with a solid-to-liquid ratio of 2.5 and 12 M of NaOH [148,191]. These values provide the highest compressive strength compared to other ratios of 1.5 and 3. The OH^- increases with the increase in the molarity of NaOH to 12, accelerating the hydrolysis and dissolution processes. In addition, the ratio of silica to alumina increases with the increase in the sodium silicate to sodium hydroxide ratio, providing strong bonds. Additionally, the intermolecular contact rate between the activator and precursor increases with the increase in the solid-to-liquid ratio to 2.5, leading to more dissolved aluminosilicates [148]. FA-based geopolymer provides a compressive strength of 47 MPa, exceeding the requirement for rigid pavement applications, with lower loss of

strength, permeability, weight loss, and susceptibility to acid attack in comparison with conventional concrete [45,192]. Thus, it is suggested to incorporate FA in geopolymer binder for rigid pavement due to its high mechanical and durability performance, though further research would be beneficial in terms of the impact on the environment, temperature, and long-term durability under harmful conditions.

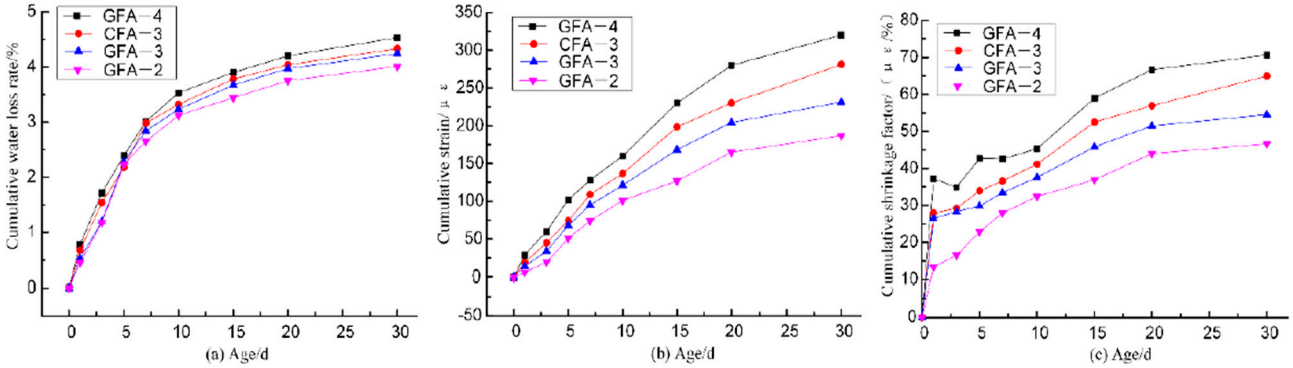

Figure 19. Effect of curing times on the durability properties of geopolymer-stabilized macadam highway [145].

A comparison was made between FA-based geopolymer concrete and conventional concrete materials for the base layer [149]. The compressive strength ranged from 10.3 to 34.9 MPa for all geopolymer samples cured for 7, 28, and 90 days. The flexural strength also increased with curing age continuously. FA geopolymer concrete was reported to have lower dry shrinkage than traditional base materials, suggesting reflective crack improvements and good performance of the pavement. The percentage increase of indirect tensile strength was about 50% from 7 to 28 days of curing, with 33 MPa resilient modulus. However, additional research on the behavior of geopolymer bases with the use of various raw materials is essential. In another study, Ojha and Lokesh [193] explored the possibility of using recycled aggregates to prepare FA-based geopolymer concrete and tested it against conventional concrete. The results showed acceptable performance of the geopolymer concrete over conventional concrete. The splitting and tensile strengths were lower than those of conventional concrete though within the permissible range.

The use of recycled waste materials in terms of RAP–S geopolymer in pavement base applications was reported by Hoy et al. [107]. The blending of S with RAP increases the maximum dry unit weight. The blending of 10% S with 10% RAP and curing for 7 days were not able to provide resistance to immersion in water for 2 h. The strength increased with the increase in curing time, though only a 1.5:1 ratio of sodium hydroxide to sodium silicate at 20% S provided adequate strength for base materials at 7 days according to the highway standards. SEM and XRD analyses showed the formation of C-S-H or C-A-S-H gels as the main products from RAP + 20% S geopolymer, with an increase in the content of C-A-S-H over time. Highly soluble silica is the main constituent of sodium silicate activator, providing a faster geopolymerization process and more hydration products when used in a suitable amount. The increase in the activator beyond the optimum level increases the silica content, retarding the rate of geopolymerization and reducing strength. Without the use of sodium silicate (i.e., 100% NaOH), a slow rate of geopolymerization occurs at room temperature. Meanwhile, Rahman and Khattak [194] conducted a series of laboratory investigations to investigate the mechanical, durability, and morphological characteristics of RAP geopolymer concrete and compared it with RAP cement concrete. Results indicated the higher performance of RAP geopolymer concrete than RAP cement concrete in terms of tensile and compressive strengths. Satisfactory resistance to wet and dry cycles, as well as water absorption, was obtained from RAP geopolymer concrete. The morphological study discovered the formation of geopolymer compounds in RAP geopolymer concrete.

Additionally, it is possible to use shredded waste plastic, waste brick aggregates, as well as clay brick waste powder (WBP) for producing MK geopolymer pavement bricks [146]. The compressive strength was from 31 to 48 MPa, which is adequate for brick construction even with the reduced strength of conventional bricks with the use of geopolymers, particularly plastic aggregates. The water absorption of the bricks was significantly reduced by the use of the geopolymer, with 15% WBP. Considering the strength, the developed pavement bricks can be categorized as having a medium–light loading capacity with minimal absorption of water from 3.7 to 5.3% with adequate resistance to abrasion and wear.

4.4. Carbon and Ecological Footprints of Geopolymers

The typical embodied carbon for a precast concrete member is shown in Figure 20. In a structural concrete element, the content of cement by mass ranges from 15 to 25%, though it is responsible for more than 75% of the total emissions of CO_2 [195]. The substitution of cement by waste materials such as GGBS and FA can significantly reduce the CO_2 emission, though cement is still responsible for a significant portion of the CO_2 emission.

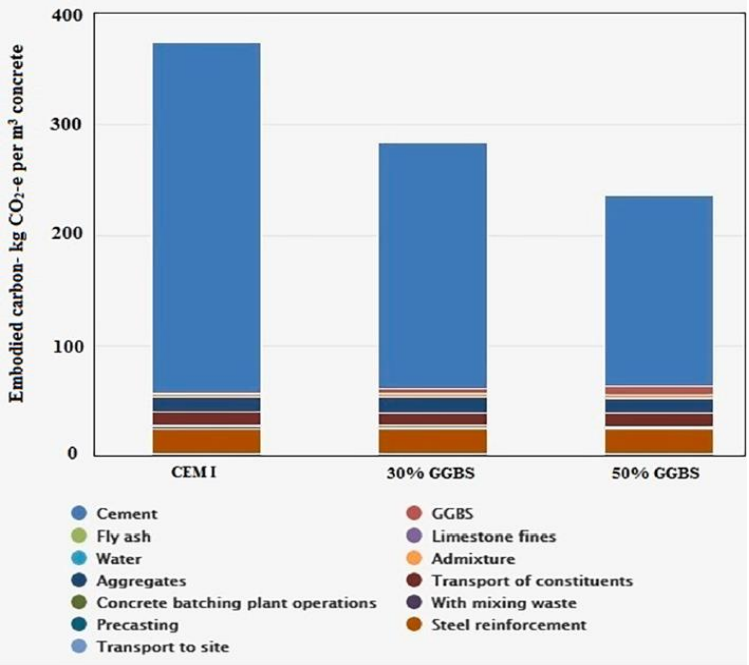

Figure 20. Embodied carbon in a precast reinforced concrete member [4,196].

Neupane [4] estimated the CO_2 emission of geopolymer binder in comparison with cement by the use of published data on the carbon footprint and embodied energy of individual constituents. For instance, Turner and Collins [197] and Heath et al. [198] suggested 1.222 kg and 0.445 kg of CO_2 emission, respectively, for the production of 1 kg of sodium silicate liquid. The summary of the literature on CO_2 emission for the individual materials of geopolymer and concrete as reported by Neupane [4] indicates that the major contributor to CO_2 emission are cement, superplasticizers, and alkaline activators, though superplasticizers have an insignificant impact since they are normally used in small amounts compared to binder and aggregates. Table 6 shows the estimation of the carbon footprint and embodied energy of geopolymer constituents as determined by Neupane [4]. The comparison between cement and geopolymer is shown in Figure 21, which indicates the significant efficiency of geopolymer in terms of carbon emission in comparison with cement. For a similar produced mass, the emission of CO_2 and the consumption of energy are lower by about five times and three times compared to cement.

Table 6. The carbon footprint of ingredients of one part of geopolymer [4].

Geopolymer						**OPC**
Ingredients kg (per kg of binder)	Fly ash	GGBS	Sodium silicate	Sodium carbonate	Total	
	0.5	0.32	0.09	0.09	1.0	
Carbon emission (kg CO_2-e/kg)	0.0135	0.0457	0.0803	0.0225	0.162	0.86
Embodied energy (MJ/kg)	0.05	0.1056	1.611	0.1215	1.888	5.6

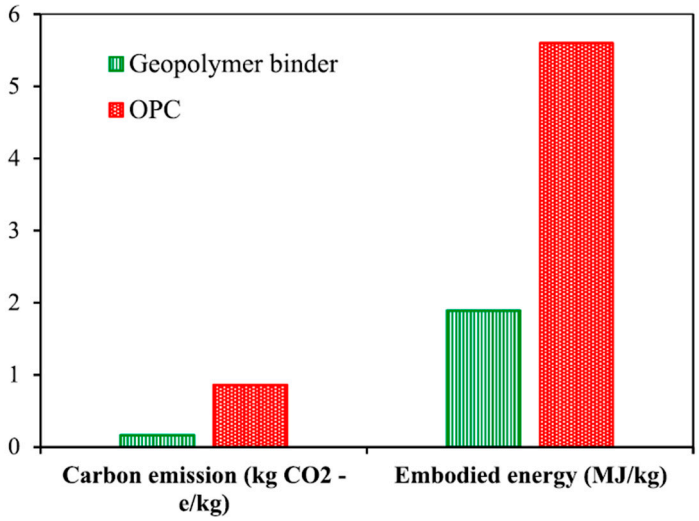

Figure 21. The carbon footprint of geopolymer and normal concrete [4].

An ecological footprint is the estimation of the biologically productive sea and land area needed for the generation or preparation of renewable resources for consumption by the population and for absorbing waste from animals and human activities. It is the total region of grazing and cropland for producing food for animals and humans, construction area for infrastructure and housing, forest land for absorbing the emitted carbon dioxide from energy consumption and for production of timber, etc. An ecological footprint is usually measured in terms of hectares of biologically productive area [199,200].

For producing concrete, the ecological footprint of the environmental impacts was studied by Akhtar et al. [127]. The investigation compares the cost and total required ecological footprints determined by various standards for the production of normal concrete and geopolymer. The results shown in Figure 22 indicate that geopolymer has a significantly lower ecological footprint in comparison with normal concrete according to all used standards. The contributions to the total ecological footprint by the constituents of concrete and the amounts of energy, labor, and machinery required for concrete production in comparison with geopolymer are shown in Figure 23. For normal concrete, about 90% of the contributions are related to the materials while labor and energy account for only 6–8% and 2–3%, respectively. Cement, among the other materials of concrete, accounts for 95% of the total contribution of the materials to the ecological footprint. On the other hand, geopolymer concrete accounts for about 46%, 10%, and 44% of materials, labor, and energy, respectively. Activators in terms of sodium silicates and sodium hydroxide are higher contributors in terms of energy for geopolymer. The difference between normal concrete and geopolymer concrete is mainly related to the cement since other materials such as water and aggregates have nearly the same ecological footprint in both. However, the heat curing required for the production of geopolymer for 24 h at 85 °C makes a noticeable contribution to the ecological footprint, which contributes to the high energy share of the geopolymer. This can be reduced by limiting the high curing temperature by the use of ambient temperature in hot and dry areas without adversely impacting the strength. The

use of hot curing chambers with renewable energy sources could be a vital alternative. Further research is required in terms of the sources of silica, activators, and curing methods for the best usage of geopolymer.

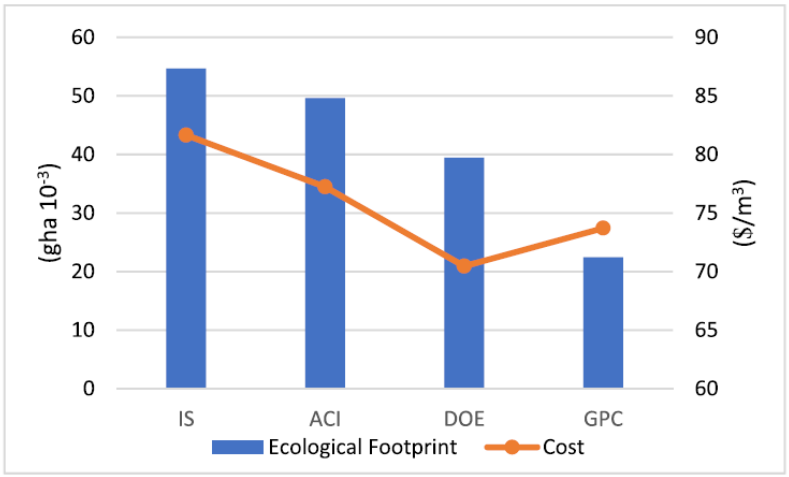

Figure 22. Ecological footprint and cost of normal concrete per various standards and FA geopolymer concrete [127].

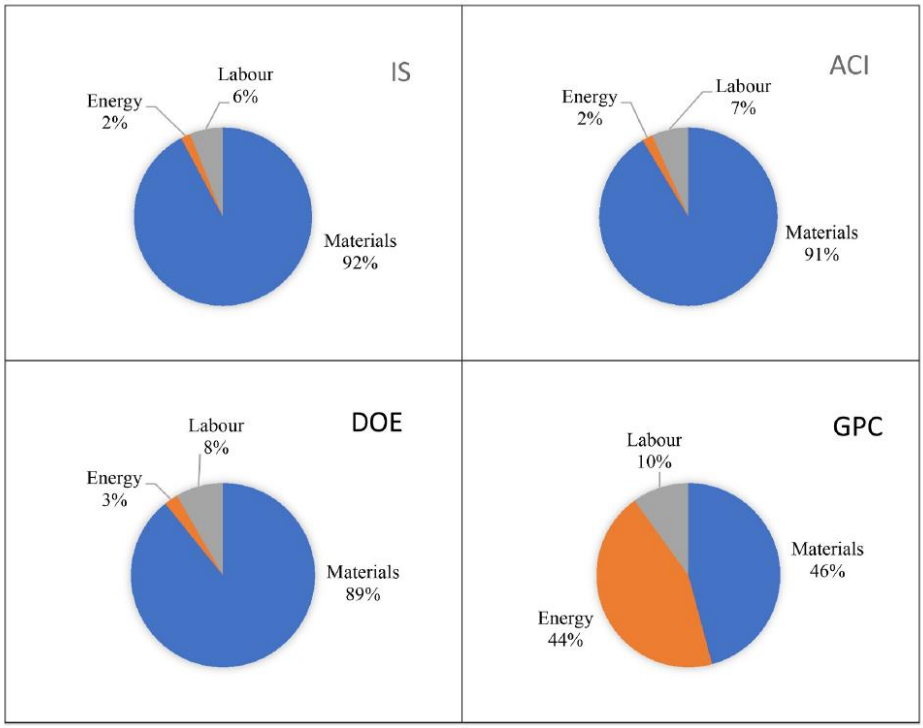

Figure 23. Share of materials, machinery, energy, and labor in total ecological footprint [127].

Akhtar et al. [127] compare the cost required for the production of normal concrete by various standards with that of FA geopolymer concrete. The production of 1 m^3 of concrete by IS, ACI, and DOE standards costs about USD 81.65, USD 77.23, and USD 73.70, respectively. Meanwhile, geopolymer concrete includes the cost of sand when produced by the DOE code, which is much lower if heat curing is limited. However, the use of by-product materials as precursors in geopolymer assists in the management and commercialization of the waste as well as reducing the number of cement requirements.

Neupane [4] estimated the sustainability of geopolymer binder in comparison with cement by the use of various studies in the literature. The comparison was conducted on

various precursors types in geopolymer binders, including GGBS-based geopolymer [201], FA-based geopolymer [202], and FA–GGBS-based geopolymer [203,204], with various activator contents and curing regimes. In general, the temperature requirements for FA-based geopolymer are significantly higher than those of GGBS-based geopolymer due to its low rate of reaction at ambient curing temperatures.

Although FA causes a very low emission of carbon, it has some sustainability issues in geopolymer-based binder since it consumes a considerable amount of energy for curing. Diaz-Loya et al. [202] reported significantly higher embodied energy of FA-based geopolymer than geopolymer cured at an ambient temperature. In normal geopolymer concrete, the main sources of carbon emission and embodied energy are the activators and coarse aggregates. At the same strength grade, FA–GGBS-based geopolymer concrete has a substantially larger sustainable footprint than only FA- or GGBS-based geopolymer concrete as it only has 50% FA content, reducing the required curing temperature.

5. Potential of Geopolymer Concrete Applications in Construction

Geopolymer technology has been considered as a promising technique to reduce or replace the use of conventional concrete by solving the emission and disposal problems from inductors such as rice milling, thermal plants, steel industries, etc. However, challenges are present in achieving comparable or better properties than conventional concrete. These include the requirement of high dosages of alkaline activators and curing temperatures [205]. Another significant challenge is the properties of raw materials such as GGBS, FA, RHA, POFA, MK, etc. It has been reported that the sources of these materials impact their properties, thereby requiring different chemical activator dosages, curing regimes, etc. Thus, mixing proportion criteria are yet to be obtained. This review revealed various parameters for various waste- and by-product-based geopolymers to bridge the gap between laboratories and actual industrial applications. Some advanced curing regimes can be developed regarding the emitted gas from industries by adjusting them to the required temperature inside the chamber where the curing is carried out. Some advanced methods such as nuclear magnetic resonance can be used under XRD that can elucidate the amorphous products formed by mixing various source materials. Furthermore, the pH of the reaction products can be studied to check their acidity or usage in conjunction with steel reinforcement or whether it is too basic to cause other deteriorations.

6. Conclusions and Perspectives

Based on the results presented and discussed in the previous sections, it is found that geopolymer has a possible utilization in various engineering fields as a construction material. Several mechanical and physical properties have been studied and evaluated by various researchers and adequate strengths were obtained. Based on ACI guidelines, most of the obtained strength levels apply to various fields. Through carbon and ecological footprint studies, the efficient and green possibility of geopolymer in terms of carbon emission, required energy for production, and the required labor and machinery was evident.

The production of geopolymer can be achieved successfully, though a better understanding of the short- and long-term mechanical characteristics and durability, the relation between the components of the mix design, and the setting reactions involved is needed. Significant improvements in the research on geopolymer have been made, however, further work is still required. These are related to bonds between aggregates and paste, aggregate- or additive-to-binder ratio, liquid-to-solid or -binder ratio, curing temperature, reinforcements and their behavior in geopolymer concrete or structural elements, etc. Traditionally, and in particular, for FA-based geopolymer, a high curing temperature is required, causing handling difficulty in the field. Thus, efforts are required for developing a system of curing at an ambient temperature for the geopolymer constituents by the use of solid activators instead of alkaline solutions. It is felt that the application of geopolymer is limited by several factors, especially the durability. Additionally, there is a lack in terms of the provision of an

appropriate code of practice for the use of geopolymer in various engineering fields, which could be formulated by the use of field and research data for users' adaptation.

Author Contributions: Conceptualization, Z.J. and A.D.; methodology, Z.J. and A.D.; software, Z.J. and A.D.; validation, Z.J., A.D. and M.A.O.M.; formal analysis, Z.J. and N.M.; investigation, Z.J, A.D., N.M. and M.A.O.M.; resources, Z.J., N.M. and A.D.; data curation, Z.J., A.D. and M.A.O.M.; writing—original draft preparation, Z.J., A.D. and N.M.; writing—review and editing, Z.J., M.A.O.M. and A.D.; visualization, Z.J.; supervision, Z.J. and A.D.; project administration, A.D. All authors have read and agreed to the published version of the manuscript.

Funding: This research received no external funding.

Institutional Review Board Statement: Not applicable.

Informed Consent Statement: Not applicable.

Data Availability Statement: Not applicable.

Acknowledgments: The financial support of the University of Warith Al-Anbiyaa in Iraq is gratefully acknowledged.

Conflicts of Interest: The authors declare no conflict of interest.

References

1. Prospects, M. Global Construction Trends. 2022. Available online: https://www.marketprospects.com/articles/global-construction-industry-trends (accessed on 1 January 2023).
2. PCA How Cement Is Made. 2019. Available online: https://www.cement.org/cement-concrete/how-cement-is-made (accessed on 26 April 2023).
3. Hendriks, C.A.; Worrell, E.; De Jager, D.; Blok KRiemer, P. Emission reduction of greenhouse gases from the cement industry. In Proceedings of the Fourth International Conference on Greenhouse Gas Control Technologies, Interlaken, Switzerland, 30 August–2 September 1998; IEA GHG R&D Programme: Interlaken, Austria, 1998.
4. Neupane, K. Evaluation of environmental sustainability of one-part geopolymer binder concrete. *Clean. Mater.* **2022**, *6*, 100138. [CrossRef]
5. Direct CO_2 Intensity of Cement Production in the Net Zero Scenario, 2015–2030. 2021. Available online: https://www.iea.org/reports/cement (accessed on 21 December 2022).
6. Van Oss, H.G.; Padovani, A.C. Cement manufacture and the environment part II: Environmental challenges and opportunities. *J. Ind. Ecol.* **2003**, *7*, 93–126.
7. Farooq, F.; Jin, X.; Faisal Javed, M.; Akbar, A.; Izhar Shah, M.; Aslam, F.; Alyousef, R. Geopolymer concrete as sustainable material: A state of the art review. *Constr. Build. Mater.* **2021**, *306*, 124762. [CrossRef]
8. Chen, C.; Habert, G.; Bouzidi, Y.; Jullien, A. Environmental impact of cement production: Detail of the different processes and cement plant variability evaluation. *J. Clean. Prod.* **2010**, *18*, 478–485. [CrossRef]
9. Carreño-Gallardo, C.; Tejeda-Ochoa, A.; Perez-Ordonez, O.I.; Ledezma-Sillas, J.E.; Lardizabal-Gutierrez, D.; Prieto-Gomez, C.; Valenzuela-Grado, J.A.; Hernandez, F.R.; Herrera-Ramirez, J.M. In the CO_2 emission remediation by means of alternative geopolymers as substitutes for cements. *J. Environ. Chem. Eng.* **2018**, *6*, 4878–4884. [CrossRef]
10. Mehta, K.P. Reducing the environmental impact of concrete. *Concr. Int.* **2001**, *23*, 61–66.
11. Suhendro, B. Toward green concrete for better sustainable environment. *Procedia Eng.* **2014**, *95*, 305–320. [CrossRef]
12. Negahban, E. *Investigation of Geopolymer Concrete for Pavement Applications*; Swinburne University of Technology: Melbourne, Australia, 2022.
13. ICR. *Global Cement Report*, 13th ed.; CemNet: Dorking, UK; International Cement Review: Dorking, UK, 2019.
14. Schneider, M.; Romer, M.; Tschudin MBolio, H. Sustainable cement production—Present and future. *Cem. Concr. Res.* **2011**, *41*, 642–650. [CrossRef]
15. Müller, N.a.J.H. *A Blueprint for a Climate-Friendly Cement Industry: How to Turn around the Trend of Cement Related Emissions in the Developing World*; World Wide Fund for Nature: Gland, Switzerland, 2008; p. 101.
16. Berry, M.; Cross, D.; Stephens, J. Changing the Environment: An Alternative " Green " Concrete Produced without Portland Cement. In Proceedings of the 2009 World of Coal Ash (WOCA) Conference, Lexington, KY, USA, 4–7 May 2009.
17. Alam, O.; Qiao, X. An in-depth review on municipal solid waste management, treatment and disposal in Bangladesh. *Sustain. Cities Soc.* **2020**, *52*, 101775. [CrossRef]
18. Patwa, A.; Parde, D.; Dohare, D.; Vijay, R.; Kumar, R. Solid waste characterization and treatment technologies in rural areas: An Indian and international review. *Environ. Technol. Innov.* **2020**, *20*, 101066. [CrossRef]
19. Kang, S.; Zhao, Y.; Wang, W.; Zhang, T.; Chen, T.; Yi, H.; Rao, F.; Song, S. Removal of methylene blue from water with montmorillonite nanosheets/chitosan hydrogels as adsorbent. *Appl. Surf. Sci.* **2018**, *448*, 203–211. [CrossRef]

20. Harbec, D.; Zidol, A.; Tagnit-Hamou, A.; Gitzhofer, F. Mechanical and durability properties of high performance glass fume concrete and mortars. *Constr. Build. Mater.* **2017**, *134*, 142–156. [CrossRef]
21. Pacewska, B.; Wilińska, I. Usage of supplementary cementitious materials: Advantages and limitations. *J. Therm. Anal. Calorim.* **2020**, *142*, 371–393. [CrossRef]
22. Fantilli, A.P.; Jóźwiak-Niedźwiedzka, D. Special Issue: Supplementary Cementitious Materials in Concrete, Part I. *Materials* **2021**, *14*, 2291. [CrossRef] [PubMed]
23. Amin, A. Application of Supplementary Cementitious Materials in Precast Concrete Industry. In *Sustainability of Concrete with Synthetic and Recycled Aggregates*; Hosam, M.S., Ed.; IntechOpen: Rijeka, Croatia, 2021; Chapter 8.
24. Jiang, X.; Zhang, Y.; Zhang, Y.; Ma, J.; Xiao, R.; Guo, F.; Bai, Y.; Huang, B. Influence of size effect on the properties of slag and waste glass-based geopolymer paste. *J. Clean. Prod.* **2023**, *383*, 135428. [CrossRef]
25. Xiao, R.; Huang, B.; Zhou, H.; Ma, Y.; Jiang, X. A state-of-the-art review of crushed urban waste glass used in OPC and AAMs (geopolymer): Progress and challenges. *Clean. Mater.* **2022**, *4*, 100083. [CrossRef]
26. Davidovits, J. 30 Years of Successes and Failures in Geopolymer Applications. Market Trends and Potential Breakthroughs. In Proceedings of the Geopolymer 2002 Conference, Melbourne, Australia, 28–29 October 2002.
27. Huang, G.; Ji, Y.; Li, J.; Hou, Z.; Jin, C. Use of slaked lime and Portland cement to improve the resistance of MSWI bottom ash-GBFS geopolymer concrete against carbonation. *Constr. Build. Mater.* **2018**, *166*, 290–300. [CrossRef]
28. Kurtoglu, A.E.; Alzeebaree, R.; Aljumaili, O.; Nis, A.; Gulsan, M.E.; Humur, G.; Cevik, A. Mechanical and durability properties of fly ash and slag based geopolymer concrete. *Adv. Concr. Constr.* **2018**, *6*, 345.
29. Mehta, A.; Siddique, R. Sustainable geopolymer concrete using ground granulated blast furnace slag and rice husk ash: Strength and permeability properties. *J. Clean. Prod.* **2018**, *205*, 49–57. [CrossRef]
30. Venkatesan, R.P.; Pazhani, K.C. Strength and durability properties of geopolymer concrete made with Ground Granulated Blast Furnace Slag and Black Rice Husk Ash. *KSCE J. Civ. Eng.* **2016**, *20*, 2384–2391. [CrossRef]
31. Adak, D.; Sarkar, M.; Mandal, S. Structural performance of nano-silica modified fly-ash based geopolymer concrete. *Constr. Build. Mater.* **2017**, *135*, 430–439. [CrossRef]
32. Jiang, X.; Xiao, R.; Zhang, M.; Hu, W.; Bai, Y.; Huang, B. A laboratory investigation of steel to fly ash-based geopolymer paste bonding behavior after exposure to elevated temperatures. *Constr. Build. Mater.* **2020**, *254*, 119267. [CrossRef]
33. Mehta, A.; Siddique, R. Sulfuric acid resistance of fly ash based geopolymer concrete. *Constr. Build. Mater.* **2017**, *146*, 136–143. [CrossRef]
34. Nuaklong, P.; Sata, V.; Chindaprasirt, P. Properties of metakaolin-high calcium fly ash geopolymer concrete containing recycled aggregate from crushed concrete specimens. *Constr. Build. Mater.* **2018**, *161*, 365–373. [CrossRef]
35. Pouhet, R.; Cyr, M. Formulation and performance of flash metakaolin geopolymer concretes. *Constr. Build. Mater.* **2016**, *120*, 150–160. [CrossRef]
36. Zhang, H.Y.; Qiu, G.H.; Kodur, V.; Yuan, Z.S. Spalling behavior of metakaolin-fly ash based geopolymer concrete under elevated temperature exposure. *Cem. Concr. Compos.* **2020**, *106*, 103483. [CrossRef]
37. Xie, T.; Ozbakkaloglu, T. Behavior of low-calcium fly and bottom ash-based geopolymer concrete cured at ambient temperature. *Ceram. Int.* **2015**, *41*, 5945–5958. [CrossRef]
38. Zabihi, S.M.; Tavakoli, H.; Mohseni, E. Engineering and microstructural properties of fiber-reinforced rice husk–ash based geopolymer concrete. *J. Mater. Civ. Eng.* **2018**, *30*, 04018183. [CrossRef]
39. Davidovits, J. Geopolymers and geopolymeric materials. *J. Therm. Anal.* **1989**, *35*, 429–441. [CrossRef]
40. Provis, J.L.; Bernal, S.A. Geopolymers and related alkali-activated materials. *Annu. Rev. Mater. Res.* **2014**, *44*, 299–327. [CrossRef]
41. De Oliveira, L.B.; de Azevedo, A.R.G.; Marvila, M.T.; Pereira, E.C.; Fediuk, R.; Vieira, C.M.F. Durability of geopolymers with industrial waste. *Case Stud. Constr. Mater.* **2022**, *16*, e00839. [CrossRef]
42. Duxson, P.; Fernández-Jiménez, A.; Provis, J.L.; Lukey, G.C.; Palomo, A.; van Deventer, J.S.J. Geopolymer technology: The current state of the art. *J. Mater. Sci.* **2007**, *42*, 2917–2933. [CrossRef]
43. Provis, J.L.; Van Deventer, J.S. *Geopolymers: Structures, Processing, Properties and Industrial Applications*; Elsevier: New York, NY, USA, 2009.
44. Unis Ahmed, H.; Mahmood, L.J.; Muhammad, M.A.; Faraj, R.H.; Qaidi, S.M.A.; Hamah Sor, N.; Mohammed, A.S.; Mohammed, A.A. Geopolymer concrete as a cleaner construction material: An overview on materials and structural performances. *Clean. Mater.* **2022**, *5*, 100111. [CrossRef]
45. Singh, N.B.; Middendorf, B. Geopolymers as an alternative to Portland cement: An overview. *Constr. Build. Mater.* **2020**, *237*, 117455. [CrossRef]
46. Garcia-Lodeiro, I.; Palomo, A.; Fernández-Jiménez, A. An overview of the chemistry of alkali-activated cement-based binders. In *Handbook of Alkali-Activated Cements, Mortars and Concretes*; Elsevier: Amsterdam, The Netherlands, 2015; pp. 19–47.
47. Hardjito, D.; Rangan, B.V. *Development and Properties of Low-Calcium Fly Ash-Based Geopolymer Concrete*; Resaerch report; Curtin University of Technology Perth: Bentley, Australia, 2005.
48. van Jaarsveld, J.G.S.; van Deventer, J.S.J.; Lukey, G.C. The characterisation of source materials in fly ash-based geopolymers. *Mater. Lett.* **2003**, *57*, 1272–1280. [CrossRef]
49. Fu, C.; Ye, H.; Zhu, K.; Fang, D.; Zhou, J. Alkali cation effects on chloride binding of alkali-activated fly ash and metakaolin geopolymers. *Cem. Concr. Compos.* **2020**, *114*, 103721. [CrossRef]

50. Ambily, P.S.; Ravisankar, K.; Umarani, C.; Dattatreya, J.K.; Iyer, N.R. Development of ultra-high-performance geopolymer concrete. *Mag. Concr. Res.* **2014**, *66*, 82–89. [CrossRef]
51. Shi, C.; Jiménez, A.F.; Palomo, A. New cements for the 21st century: The pursuit of an alternative to Portland cement. *Cem. Concr. Res.* **2011**, *41*, 750–763. [CrossRef]
52. Petermann, J.C.; Saeed, A.; Hammons, M.I. *Alkali-Activated Geopolymers: A Literature Review*; Applied Research Associates Inc.: Panama City, FL, USA, 2010.
53. Rangan, B.V. *11—Engineering Properties of Geopolymer Concrete in Geopolymers*; Provis, J.L., van Deventer, J.S.J., Eds.; Woodhead Publishing: Sawston, UK, 2009; pp. 211–226.
54. Cheah, C.B.; Samsudin, M.H.; Ramli, M.; Part, W.K.; Tan, L.E. The use of high calcium wood ash in the preparation of Ground Granulated Blast Furnace Slag and Pulverized Fly Ash geopolymers: A complete microstructural and mechanical characterization. *J. Clean. Prod.* **2017**, *156*, 114–123. [CrossRef]
55. Fernández-Jiménez, A.; Vallepu, R.; Terai, T.; Palomo, A.; Ikeda, K. Synthesis and thermal behavior of different aluminosilicate gels. *J. Non-Cryst. Solids* **2006**, *352*, 2061–2066. [CrossRef]
56. Duxson, P.; Provis, J.L.; Lukey, G.C.; Van Deventer, J.S. The role of inorganic polymer technology in the development of 'green concrete'. *Cem. Concr. Res.* **2007**, *37*, 1590–1597. [CrossRef]
57. Zhang, D.-W.; Wang, D.-m.; Liu, Z.; Xie, F.-z. Rheology, agglomerate structure, and particle shape of fresh geopolymer pastes with different NaOH activators content. *Constr. Build. Mater.* **2018**, *187*, 674–680. [CrossRef]
58. Cong, P.; Cheng, Y. Advances in geopolymer materials: A comprehensive review. *J. Traffic Transp. Eng. (Engl. Ed.)* **2021**, *8*, 283–314. [CrossRef]
59. Singh, N.B. Fly ash-based geopolymer binder: A future construction material. *Minerals* **2018**, *8*, 299. [CrossRef]
60. Provis, J.L.; Lukey, G.C.; van Deventer, J.S. Do geopolymers actually contain nanocrystalline zeolites? A reexamination of existing results. *Chem. Mater.* **2005**, *17*, 3075–3085. [CrossRef]
61. Ranjbar, N.; Kuenzel, C.; Spangenberg, J.; Mehrali, M. Hardening evolution of geopolymers from setting to equilibrium: A review. *Cem. Concr. Compos.* **2020**, *114*, 103729. [CrossRef]
62. Zhao, M.; Zhang, G.; Htet, K.W.; Kwon, M.; Liu, C.; Xu, Y.; Tao, M. Freeze-thaw durability of red mud slurry-class F fly ash-based geopolymer: Effect of curing conditions. *Constr. Build. Mater.* **2019**, *215*, 381–390. [CrossRef]
63. Yip, C.K.; Lukey, G.C.; van Deventer, J.S.J. The coexistence of geopolymeric gel and calcium silicate hydrate at the early stage of alkaline activation. *Cem. Concr. Res.* **2005**, *35*, 1688–1697. [CrossRef]
64. van Overmeir, A.L.; Figueiredo, S.C.; Šavija, B.; Bos, F.P.; Schlangen, E. Design and analyses of printable strain hardening cementitious composites with optimized particle size distribution. *Constr. Build. Mater.* **2022**, *324*, 126411. [CrossRef]
65. Pacheco-Torgal, F.; Labrincha, J.; Leonelli, C.; Palomo, A.; Chindaprasit, P. *Handbook of Alkali-Activated Cements, Mortars and Concretes*; Elsevier: Amsterdam, The Netherlands, 2014.
66. Nath, P. Study of fly ash based geopolymer concrete cured in ambient condition. In *School of Civil and Mechanical Engineering*; Curtin University: Perth, Australia, 2014.
67. Kadhim, A.; Sadique, M.; Al-Mufti, R.; Hashim, K. Developing one-part alkali-activated metakaolin/natural pozzolan binders using lime waste. *Adv. Cem. Res.* **2021**, *33*, 342–356. [CrossRef]
68. Granizo, N.; Palomo, A.; Fernandez-Jiménez, A. Effect of temperature and alkaline concentration on metakaolin leaching kinetics. *Ceram. Int.* **2014**, *40*, 8975–8985. [CrossRef]
69. Khalid, H.R.; Lee, N.K.; Park, S.M.; Abbas, N.; Lee, H.K. Synthesis of geopolymer-supported zeolites via robust one-step method and their adsorption potential. *J. Hazard. Mater.* **2018**, *353*, 522–533. [CrossRef] [PubMed]
70. Barbosa, T.R.; Foletto, E.L.; Dotto, G.L.; Jahn, S.L. Preparation of mesoporous geopolymer using metakaolin and rice husk ash as synthesis precursors and its use as potential adsorbent to remove organic dye from aqueous solutions. *Ceram. Int.* **2018**, *44*, 416–423. [CrossRef]
71. Lee, N.; Khalid, H.R.; Lee, H.-K. Synthesis of mesoporous geopolymers containing zeolite phases by a hydrothermal treatment. *Microporous Mesoporous Mater.* **2016**, *229*, 22–30. [CrossRef]
72. Khale, D.; Chaudhary, R. Mechanism of geopolymerization and factors influencing its development: A review. *J. Mater. Sci.* **2007**, *42*, 729–746. [CrossRef]
73. Wongsa, A.; Siriwattanakarn, A.; Nuaklong, P.; Sata, V.; Sukontasukkul, P.; Chindaprasirt, P. Use of recycled aggregates in pressed fly ash geopolymer concrete. *Environ. Prog. Sustain. Energy* **2020**, *39*, e13327. [CrossRef]
74. Provis, J.L.; Yong, S.L.; Duxson, P. *5—Nanostructure/Microstructure of Metakaolin Geopolymers in Geopolymers*; Provis, J.L., van Deventer, J.S.J., Eds.; Woodhead Publishing: Sawston, UK, 2009; pp. 72–88.
75. Garcia-Lodeiro, I.; Palomo, A.; Fernández-Jiménez, A.; Macphee, D.E. Compatibility studies between, N-A-S-H and C-A-S-H gels. Study in the ternary diagram, Na_2O–CaO–Al_2O_3–SiO_2–H_2O. *Cem. Concr. Res.* **2011**, *41*, 923–931. [CrossRef]
76. Nagajothi, S.; Elavenil, S. Effect of GGBS Addition on Reactivity and Microstructure Properties of Ambient Cured Fly Ash Based Geopolymer Concrete. *Silicon* **2021**, *13*, 507–516. [CrossRef]
77. Al Nageim, H.; Dulaimi, A.; Ruddock, F.; Seton, L. Development of a new cementitious filler for use in fast-curing cold binder course in pavement application. In Proceedings of the 38th International Conference on Cement Microscopy, Lyon, France, 17–21 April 2016; pp. 167–180.

78. Terzano, R.; Spagnuolo, M.; Medici, L.; Tateo, F.; Ruggiero, P. Characterization of different coal fly ashes for their application in the synthesis of zeolite X as cation exchanger for soil remediation. *Fresenius Environ. Bull.* **2005**, *14*, 263–267.
79. Castel, A.; Foster, S.J. Bond strength between blended slag and Class F fly ash geopolymer concrete with steel reinforcement. *Cem. Concr. Res.* **2015**, *72*, 48–53. [CrossRef]
80. Couto Mantese, G.; Capaldo Amaral, D. Comparison of industrial symbiosis indicators through agent-based modeling. *J. Clean. Prod.* **2017**, *140*, 1652–1671. [CrossRef]
81. Dulaimi, A.; Al Nageim, H.; Ruddock, F.; Seton, L. Assessment the Performance of Cold Bituminous Emulsion Mixtures with Cement and Supplementary Cementitious Material for Binder Course Mixture. In Proceedings of the 38th International Conference on Cement Microscopy, Lyon, France, 17–21 April 2016; pp. 283–296.
82. Poudenx, P. The effect of transportation policies on energy consumption and greenhouse gas emission from urban passenger transportation. *Transp. Res. Part A Policy Pract.* **2008**, *42*, 901–909. [CrossRef]
83. Ukwattage, N.L.; Ranjith, P.G.; Bouazza, M. The use of coal combustion fly ash as a soil amendment in agricultural lands (with comments on its potential to improve food security and sequester carbon). *Fuel* **2013**, *109*, 400–408. [CrossRef]
84. Mahvash, S.; López-Querol, S.; Bahadori-Jahromi, A. Effect of class F fly ash on fine sand compaction through soil stabilization. *Heliyon* **2017**, *3*, e00274. [CrossRef] [PubMed]
85. Kobayashi, Y.; Ogata, F.; Nakamura, T.; Kawasaki, N. Synthesis of novel zeolites produced from fly ash by hydrothermal treatment in alkaline solution and its evaluation as an adsorbent for heavy metal removal. *J. Environ. Chem. Eng.* **2020**, *8*, 103687. [CrossRef]
86. Schönegger, D.; Gómez-Brandón, M.; Mazzier, T.; Insam, H.; Hermanns, R.; Leijenhorst, E.; Bardelli, T.; Juárez, M.F.-D. Phosphorus fertilising potential of fly ash and effects on soil microbiota and crop. *Resour. Conserv. Recycl.* **2018**, *134*, 262–270. [CrossRef]
87. Dulaimi, A.; Al-Busaltan, S.; Sadique, M. The development of a novel, microwave assisted, half-warm mixed asphalt. *Constr. Build. Mater.* **2021**, *301*, 124043. [CrossRef]
88. Ahmad, J.; Kontoleon, K.J.; Majdi, A.; Naqash, M.T.; Deifalla, A.F.; Ben Kahla, N.; Isleem, H.F.; Qaidi, S.M. A comprehensive review on the ground granulated blast furnace slag (GGBS) in concrete production. *Sustainability* **2022**, *14*, 8783. [CrossRef]
89. Dulaimi, A.; Shanbara, H.K.; Al-Rifaie, A. The mechanical evaluation of cold asphalt emulsion mixtures using a new cementitious material comprising ground-granulated blast-furnace slag and a calcium carbide residue. *Constr. Build. Mater.* **2020**, *250*, 118808. [CrossRef]
90. He, J.; Zhang, J.; Yu, Y.; Zhang, G. The strength and microstructure of two geopolymers derived from metakaolin and red mud-fly ash admixture: A comparative study. *Constr. Build. Mater.* **2012**, *30*, 80–91. [CrossRef]
91. Irfan Khan, M.; Khan, H.U.; Azizli, K.; Sufian, S.; Man, Z.; Siyal, A.A.; Muhammad, N.; Faiz ur Rehman, M. The pyrolysis kinetics of the conversion of Malaysian kaolin to metakaolin. *Appl. Clay Sci.* **2017**, *146*, 152–161. [CrossRef]
92. Paiva, H.; Velosa, A.; Cachim, P.; Ferreira, V.M. Effect of pozzolans with different physical and chemical characteristics on concrete properties. *Mater. Constr.* **2016**, *66*, e083. [CrossRef]
93. Mehta, A.; Siddique, R. An overview of geopolymers derived from industrial by-products. *Constr. Build. Mater.* **2016**, *127*, 183–198. [CrossRef]
94. Mir, N.; Khan, S.A.; Kul, A.; Sahin, O.; Sahmaran, M.; Koç, M. Construction and demolition waste-based geopolymers for built-environment: An environmental sustainability assessment. *Mater. Today Proc.* **2022**, *70*, 358–362. [CrossRef]
95. Sumesh, M.; Alengaram, U.J.; Jumaat, M.Z.; Mo, K.H.; Alnahhal, M.F. Incorporation of nano-materials in cement composite and geopolymer based paste and mortar–A review. *Constr. Build. Mater.* **2017**, *148*, 62–84. [CrossRef]
96. Duan, W.; Zhuge, Y.; Chow, C.W.K.; Keegan, A.; Liu, Y.; Siddique, R. Mechanical performance and phase analysis of an eco-friendly alkali-activated binder made with sludge waste and blast-furnace slag. *J. Clean. Prod.* **2022**, *374*, 134024. [CrossRef]
97. Lao, J.-C.; Xu, L.-Y.; Huang, B.-T.; Dai, J.-G.; Shah, S.P. Strain-hardening Ultra-High-Performance Geopolymer Concrete (UHPGC): Matrix design and effect of steel fibers. *Compos. Commun.* **2022**, *30*, 101081. [CrossRef]
98. Liu, Q.; Cui, M.; Li, X.; Wang, J.; Wang, Z.; Li, L.; Lyu, X. Alkali-hydrothermal activation of mine tailings to prepare one-part geopolymer: Activation mechanism, workability, strength, and hydration reaction. *Ceram. Int.* **2022**, *48*, 30407–30417. [CrossRef]
99. Zhang, R.; Zhang, Y.; Liu, T.; Wan, Q.; Zheng, D. Immobilization of vanadium and nickel in spent fluid catalytic cracking (SFCC) catalysts-based geopolymer. *J. Clean. Prod.* **2022**, *332*, 130112. [CrossRef]
100. Zhao, Q.; Ma, C.; Huang, B.; Lu, X. Development of alkali activated cementitious material from sewage sludge ash: Two-part and one-part geopolymer. *J. Clean. Prod.* **2023**, *384*, 135547. [CrossRef]
101. Oyebisi, S.; Olutoge, F.; Kathirvel, P.; Oyaotuderekumor, I.; Lawanson, D.; Nwani, J.; Ede, A.; Kaze, R. Sustainability assessment of geopolymer concrete synthesized by slag and corncob ash. *Case Stud. Constr. Mater.* **2022**, *17*, e01665. [CrossRef]
102. Oluwafemi, J.; Ofuyatan, O.; Adedeji, A.; Bankole, D.; Justin, L. Reliability assessment of ground granulated blast furnace slag/cow bone ash-based geopolymer concrete. *J. Build. Eng.* **2023**, *64*, 105620. [CrossRef]
103. Ruiz, G.; Aguilar, R.; Nakamatsu, J.; Kim, S. Synthesis of a geopolymer binders using spent fluid catalytic cracking (FCC) catalyst. *IOP Conf. Ser. Mater. Sci. Eng.* **2019**, *660*, 012009. [CrossRef]
104. Salami, B.A.; Johari, M.A.M.; Ahmad, Z.A.; Maslehuddin, M. Durability performance of palm oil fuel ash-based engineered alkaline-activated cementitious composite (POFA-EACC) mortar in sulfate environment. *Constr. Build. Mater.* **2017**, *131*, 229–244. [CrossRef]
105. Rovnaník, P.; Řezník, B.; Rovnaníková, P. Blended Alkali-activated Fly Ash/Brick Powder Materials. *Procedia Eng.* **2016**, *151*, 108–113. [CrossRef]

106. Du, C.; Yang, Q. Experimental study of the feasibility of using calcium carbide residue as an alkaline activator for clay-plant ash geopolymer. *Constr. Build. Mater.* **2021**, *301*, 124351. [CrossRef]
107. Hoy, M.; Horpibulsuk, S.; Arulrajah, A.; Mohajerani, A. Strength and microstructural study of recycled asphalt pavement: Slag geopolymer as a pavement base material. *J. Mater. Civ. Eng.* **2018**, *30*, 04018177. [CrossRef]
108. Vijaya Rangan, B. Fly Ash-Based Geopolymer Concrete. 2021. Available online: http://www.yourbuilding.org/display/yb/Fly+Ash-Based+Geopolymer+Concrete (accessed on 20 January 2023).
109. Rangan, B.V.; Hardjito, D.; Wallah, S.E.; Sumajouw, D. Studies on fly ash-based geopolymer concrete. In Proceedings of the World Congress Geopolymer, Saint Quentin, France, 28 June–1 July 2005.
110. Togibasa, O.; Mumfaijah, M.; Allo, Y.K.; Dahlan, K.; Ansanay, Y.O. The Effect of Chemical Activating Agent on the Properties of Activated Carbon from Sago Waste. *Appl. Sci.* **2021**, *11*, 11640. [CrossRef]
111. Mohamedkhair, A.K.; Aziz, M.A.; Shah, S.S.; Shaikh, M.N.; Jamil, A.K.; Qasem, M.A.A.; Buliyaminu, I.A.; Yamani, Z.H. Effect of an activating agent on the physicochemical properties and supercapacitor performance of naturally nitrogen-enriched carbon derived from Albizia procera leaves. *Arab. J. Chem.* **2020**, *13*, 6161–6173. [CrossRef]
112. Kong, D.L.Y.; Sanjayan, J.G. Damage behavior of geopolymer composites exposed to elevated temperatures. *Cem. Concr. Compos.* **2008**, *30*, 986–991. [CrossRef]
113. Jais, F.M.; Chee, C.Y.; Ismail, Z.; Ibrahim, S. Experimental design via NaOH activation process and statistical analysis for activated sugarcane bagasse hydrochar for removal of dye and antibiotic. *J. Environ. Chem. Eng.* **2021**, *9*, 104829. [CrossRef]
114. Garcia Lodeiro, I.; Cristelo, N.; Palomo, A.; Fernández-Jiménez, A. Use of industrial by-products as alkaline cement activators. *Constr. Build. Mater.* **2020**, *253*, 119000. [CrossRef]
115. Hafizuddin, M.S.; Lee, C.L.; Chin, K.L.; H'ng, P.S.; Khoo, P.S.; Rashid, U. Fabrication of Highly Microporous Structure Activated Carbon via Surface Modification with Sodium Hydroxide. *Polymers* **2021**, *13*, 3954. [CrossRef] [PubMed]
116. Lv, Y.; Zhang, F.; Dou, Y.; Zhai, Y.; Wang, J.; Liu, H.; Xia, Y.; Tu, B.; Zhao, D. A comprehensive study on KOH activation of ordered mesoporous carbons and their supercapacitor application. *J. Mater. Chem.* **2012**, *22*, 93–99. [CrossRef]
117. Siregar, G.M.; Syahputra, R.F.; Farma, R. KOH Activation with Microwave Irradiation and its Effect on the Physical Properties of Orange Peel Activated Carbon. *J. Phys. Conf. Ser.* **2021**, *2049*, 012025.
118. Fernández-Jiménez, A.; Palomo, A.; Criado, M. Microstructure development of alkali-activated fly ash cement: A descriptive model. *Cem. Concr. Res.* **2005**, *35*, 1204–1209. [CrossRef]
119. Matsimbe, J.; Dinka, M.; Olukanni, D.; Musonda, I. Geopolymer: A Systematic Review of Methodologies. *Materials* **2022**, *15*, 6852. [CrossRef]
120. Kwek, S.Y.; Awang, H.; Cheah, C.B. Influence of Liquid-to-Solid and Alkaline Activator (Sodium Silicate to Sodium Hydroxide) Ratios on Fresh and Hardened Properties of Alkali-Activated Palm Oil Fuel Ash Geopolymer. *Materials* **2021**, *14*, 4253. [CrossRef]
121. Liu, M.; Hu, B.; Zhang, C.; Wang, Q.; Sun, Z.; He, P.; Chen, Y.; Chen, D.; Zhu, J. Effect of sodium silicate on the flotation separation of chalcopyrite and galena using sodium sulfite and sulfonated lignin as depressant. *Miner. Eng.* **2022**, *182*, 107563. [CrossRef]
122. Provis, J.L.; Rees, C.A. *7—Geopolymer synthesis kinetics in Geopolymers*; Provis, J.L., van Deventer, J.S.J., Eds.; Woodhead Publishing: Sawston, UK, 2009; pp. 118–136.
123. Provis, J.L.; Deventer, J.S.J.v. *Alkali Activated Materials: State-of-the-Art Report, RILEM TC 224-AAM*; Springer: Berlin/Heidelberg, Germany, 2014.
124. Kan, L.-l.; Wang, W.-s.; Liu, W.-d.; Wu, M. Development and characterization of fly ash based PVA fiber reinforced Engineered Geopolymer Composites incorporating metakaolin. *Cem. Concr. Compos.* **2020**, *108*, 103521. [CrossRef]
125. Rathinam, K.; Sakthivel, S.; Vigneshwaran, S.; Vinayagamoorthy, M.; Kumar, N. Properties of nano silica modified cement less geopolymer composite mortar using fly ash, GGBS. *Mater. Today Proc.* **2022**, *62*, 535–542. [CrossRef]
126. Migunthanna, J.; Rajeev, P.; Sanjayan, J. Investigation of waste clay brick as partial replacement of geopolymer binders for rigid pavement application. *Constr. Build. Mater.* **2021**, *305*, 124787. [CrossRef]
127. Akhtar, N.; Ahmad, T.; Husain, D.; Majdi, A.; Alam, M.T.; Husain, N.; Wayal, A.K.S. Ecological footprint and economic assessment of conventional and geopolymer concrete for sustainable construction. *J. Clean. Prod.* **2022**, *380*, 134910. [CrossRef]
128. Jumaa, N.H.; Ali, I.M.; Nasr, M.S.; Falah, M.W. Strength and microstructural properties of binary and ternary blends in fly ash-based geopolymer concrete. *Case Stud. Constr. Mater.* **2022**, *17*, e01317. [CrossRef]
129. Alrefaei, Y.; Dai, J.-G. Tensile behavior and microstructure of hybrid fiber ambient cured one-part engineered geopolymer composites. *Constr. Build. Mater.* **2018**, *184*, 419–431. [CrossRef]
130. Kan, L.; Wang, F.; Zhang, Z.; Kabala, W.; Zhao, Y. Mechanical properties of high ductile alkali-activated fiber reinforced composites with different curing ages. *Constr. Build. Mater.* **2021**, *306*, 124833. [CrossRef]
131. Beltrame, N.A.M.; Angulski da Luz, C.; Perardt, M.; Hooton, R.D. Alkali activated cement made from blast furnace slag generated by charcoal: Resistance to attack by sodium and magnesium sulfates. *Constr. Build. Mater.* **2020**, *238*, 117710. [CrossRef]
132. Wang, Y.; Wang, Y.; Zhang, M. Effect of sand content on engineering properties of fly ash-slag based strain hardening geopolymer composites. *J. Build. Eng.* **2021**, *34*, 101951. [CrossRef]
133. Choi, S.-J.; Choi, J.-I.; Song, J.-K.; Lee, B.Y. Rheological and mechanical properties of fiber-reinforced alkali-activated composite. *Constr. Build. Mater.* **2015**, *96*, 112–118. [CrossRef]
134. Al-Rkaby, A.H.; Odeh, N.A.; Sabih, A.; Odah, H. Geotechnical characterization of sustainable geopolymer improved soil. *J. Mech. Behav. Mater.* **2022**, *31*, 484–491. [CrossRef]

135. Othman, S.; Abbas, J.M. Stabilization soft Clay Soil using Metakaolin based Geopolymer. *Diyala J. Eng. Sci.* **2021**, *14*, 131–140. [CrossRef]
136. Suksiripattanapong, C.; Tuntawoot, N.; Thumrongvut, J.; Wonglakorn, N.; Chongutsah, S.; Tabyang, W. Compressive Strength of Marginal Lateritic Soil Stabilized with Bottom Ash Geopolymer as a Pavement Material. *Int. J. Eng. Technol.* **2019**, *11*, 177–180. [CrossRef]
137. Swain, K. *Stabilization of Soil Using Geopolymer and Biopolymer*; National Institute Of Technology: Rourkela, India, 2015.
138. Hanegbi, N.; Katra, I. A clay-based geopolymer in loess soil stabilization. *Appl. Sci.* **2020**, *10*, 2608. [CrossRef]
139. Radovic, M.; Puppala, A.J. *Development of Geopolymers Based Cement and Soil Stabilizers for Transportation Infrastructure*; Transportation Consortium of South-Central States: Taylor Hall; Louisiana State University: Baton Rouge, LA, USA, 2019.
140. Wang, S.; Su, J.; Wu, Z.; Ma, W.; Li, Y.; Hui, H. Silty Clay Stabilization Using Metakaolin-Based Geopolymer Binder. *Front. Phys.* **2021**, *9*, 769786. [CrossRef]
141. Noolu, V.; Rao, G.M.; Chavali, R.V.P. Strength and durability characteristics of GGBS geopolymer stabilized black cotton soil. *Mater. Today Proc.* **2021**, *43*, 2373–2376. [CrossRef]
142. Sargent, P.; Hughes, P.N.; Rouainia, M.; White, M.L. The use of alkali activated waste binders in enhancing the mechanical properties and durability of soft alluvial soils. *Eng. Geol.* **2013**, *152*, 96–108. [CrossRef]
143. Cristelo, N.; Glendinning, S.; Teixeira Pinto, A. Deep soft soil improvement by alkaline activation. *Proc. Inst. Civ. Eng.-Ground Improv.* **2011**, *164*, 73–82. [CrossRef]
144. Hamid, A.; Alfaidi, H.; Baaj, H.; El-Hakim, M. Evaluating fly ash-based geopolymers as a modifier for asphalt binders. *Adv. Mater. Sci. Eng.* **2020**, *2020*, 1–11. [CrossRef]
145. Yue, J.; Nie, X.; Wang, Z.; Liu, J.; Huang, Y. Research on the Pavement Performance of Slag/Fly Ash-Based Geopolymer-Stabilized Macadam. *Appl. Sci.* **2022**, *12*, 10000. [CrossRef]
146. Khalil, W.I.; Frayyeh, Q.J.; Ahmed, M.F. Characteristics of eco-friendly metakaolin based geopolymer concrete pavement bricks. *Eng. Technol. J.* **2020**, *38*, 1706–1716. [CrossRef]
147. Gargav, A.; Chauhan, J.S. Role of Geopolymer Concrete for the Construction of Rigid Pavement. *Int. J. Eng. Dev. Res.* **2016**, *4*, 473–476.
148. Tahir, M.F.M.; Abdullah, M.M.A.B.; Rahim, S.Z.A.; Mohd Hasan, M.R.; Sandu, A.V.; Vizureanu, P.; Ghazali, C.M.R.; Kadir, A.A. Mechanical and Durability Analysis of Fly Ash Based Geopolymer with Various Compositions for Rigid Pavement Applications. *Materials* **2022**, *15*, 3458. [CrossRef] [PubMed]
149. Sofri, L.A.; Abdullah, M.M.A.B.; Sandu, A.V.; Imjai, T.; Vizureanu, P.; Hasan, M.R.M.; Almadani, M.; Aziz, I.H.A.; Rahman, F.A. Mechanical Performance of Fly Ash Based Geopolymer (FAG) as Road Base Stabilizer. *Materials* **2022**, *15*, 7242. [CrossRef] [PubMed]
150. Li, V.C. *Engineered Cementitious Composites (ECC): Bendable Concrete for Sustainable and Resilient Infrastructure*; Engineered Cementitious Composites (ECC); Springer: Berlin/Heidelberg, Germany, 2019.
151. Wille, K.; El-Tawil, S.; Naaman, A.E. Properties of strain hardening ultra high performance fiber reinforced concrete (UHP-FRC) under direct tensile loading. *Cem. Concr. Compos.* **2014**, *48*, 53–66. [CrossRef]
152. Kondepudi, K.; Subramaniam, K.V.L.; Nematollahi, B.; Bong, S.H.; Sanjayan, J. Study of particle packing and paste rheology in alkali activated mixtures to meet the rheology demands of 3D Concrete Printing. *Cem. Concr. Compos.* **2022**, *131*, 104581. [CrossRef]
153. Zhang, J.; Gong, C.; Guo, Z.; Zhang, M. Engineered cementitious composite with characteristic of low drying shrinkage. *Cem. Concr. Res.* **2009**, *39*, 303–312. [CrossRef]
154. Ye, N.; Yang, J.; Liang, S.; Hu, Y.; Hu, J.; Xiao, B.; Huang, Q. Synthesis and strength optimization of one-part geopolymer based on red mud. *Constr. Build. Mater.* **2016**, *111*, 317–325. [CrossRef]
155. Peng, M.X.; Wang, Z.H.; Xiao, Q.G.; Song, F.; Xie, W.; Yu, L.C.; Huang, H.W.; Yi, S.J. Effects of alkali on one-part alkali-activated cement synthesized by calcining bentonite with dolomite and Na_2CO_3. *Appl. Clay Sci.* **2017**, *139*, 64–71. [CrossRef]
156. Moukannaa, S.; Loutou, M.; Benzaazoua, M.; Vitola, L.; Alami, J.; Hakkou, R. Recycling of phosphate mine tailings for the production of geopolymers. *J. Clean. Prod.* **2018**, *185*, 891–903. [CrossRef]
157. Wei, B.; Zhang, Y.; Bao, S. Preparation of geopolymers from vanadium tailings by mechanical activation. *Constr. Build. Mater.* **2017**, *145*, 236–242. [CrossRef]
158. Tian, X.; Xu, W.; Song, S.; Rao, F.; Xia, L. Effects of curing temperature on the compressive strength and microstructure of copper tailing-based geopolymers. *Chemosphere* **2020**, *253*, 126754. [CrossRef] [PubMed]
159. Tchadjié, L.N.; Djobo, J.N.Y.; Ranjbar, N.; Tchakouté, H.K.; Kenne, B.B.D.; Elimbi, A.; Njopwouo, D. Potential of using granite waste as raw material for geopolymer synthesis. *Ceram. Int.* **2016**, *42*, 3046–3055. [CrossRef]
160. Kouamo Tchakoute, H.; Elimbi, A.; Diffo Kenne, B.B.; Mbey, J.A.; Njopwouo, D. Synthesis of geopolymers from volcanic ash via the alkaline fusion method: Effect of Al_2O_3/Na_2O molar ratio of soda–volcanic ash. *Ceram. Int.* **2013**, *39*, 269–276. [CrossRef]
161. Long, W.-J.; Xiao, B.-X.; Gu, Y.-C.; Xing, F. Micro- and macro-scale characterization of nano-SiO2 reinforced alkali activated slag composites. *Mater. Charact.* **2018**, *136*, 111–121. [CrossRef]
162. Deb, P.S.; Sarker, P.K.; Barbhuiya, S. Effects of nano-silica on the strength development of geopolymer cured at room temperature. *Constr. Build. Mater.* **2015**, *101*, 675–683. [CrossRef]

163. Wong, C.L.; Mo, K.H.; Alengaram, U.J.; Yap, S.P. Mechanical strength and permeation properties of high calcium fly ash-based geopolymer containing recycled brick powder. *J. Build. Eng.* **2020**, *32*, 101655. [CrossRef]
164. Zhang, R.; Liu, T.; Zhang, Y.; Cai, Z.; Yuan, Y. Preparation of spent fluid catalytic cracking catalyst-metakaolin based geopolymer and its process optimization through response surface method. *Constr. Build. Mater.* **2020**, *264*, 120727. [CrossRef]
165. Guo, L.; Wu, Y.; Xu, F.; Song, X.; Ye, J.; Duan, P.; Zhang, Z. Sulfate resistance of hybrid fiber reinforced metakaolin geopolymer composites. *Compos. Part B Eng.* **2020**, *183*, 107689. [CrossRef]
166. Khadka, S.D.; Jayawickrama, P.W.; Senadheera, S.; Segvic, B. Stabilization of highly expansive soils containing sulfate using metakaolin and fly ash based geopolymer modified with lime and gypsum. *Transp. Geotech.* **2020**, *23*, 100327. [CrossRef]
167. Khan, H.A.; Castel, A.; Khan, M.S. Corrosion investigation of fly ash based geopolymer mortar in natural sewer environment and sulphuric acid solution. *Corros. Sci.* **2020**, *168*, 108586. [CrossRef]
168. Lahoti, M.; Tan, K.H.; Yang, E.-H. A critical review of geopolymer properties for structural fire-resistance applications. *Constr. Build. Mater.* **2019**, *221*, 514–526. [CrossRef]
169. Yuan, Y.; Zhao, R.; Li, R.; Wang, Y.; Cheng, Z.; Li, F.; Ma, Z.J. Frost resistance of fiber-reinforced blended slag and Class F fly ash-based geopolymer concrete under the coupling effect of freeze-thaw cycling and axial compressive loading. *Constr. Build. Mater.* **2020**, *250*, 118831. [CrossRef]
170. Zhao, R.; Yuan, Y.; Cheng, Z.; Wen, T.; Li, J.; Li, F.; Ma, Z.J. Freeze-thaw resistance of Class F fly ash-based geopolymer concrete. *Constr. Build. Mater.* **2019**, *222*, 474–483. [CrossRef]
171. Chen, K.; Wu, D.; Xia, L.; Cai, Q.; Zhang, Z. Geopolymer concrete durability subjected to aggressive environments–A review of influence factors and comparison with ordinary Portland cement. *Constr. Build. Mater.* **2021**, *279*, 122496. [CrossRef]
172. Yang, T.; Yao, X.; Zhang, Z. Quantification of chloride diffusion in fly ash–slag-based geopolymers by X-ray fluorescence (XRF). *Constr. Build. Mater.* **2014**, *69*, 109–115. [CrossRef]
173. Gunasekara, C.; Law, D.; Bhuiyan, S.; Setunge, S.; Ward, L. Chloride induced corrosion in different fly ash based geopolymer concretes. *Constr. Build. Mater.* **2019**, *200*, 502–513. [CrossRef]
174. Bhardwaj, P.; Gupta, R.; Mishra, D.; Sanghi, S.; Verma, S.; Amritphale, S.S. Corrosion and fire protective behavior of advanced phosphatic geopolymeric coating on mild steel substrate. *Silicon* **2020**, *12*, 487–500. [CrossRef]
175. Law, D.W.; Adam, A.A.; Molyneaux, T.K.; Patnaikuni, I.; Wardhono, A. Long term durability properties of class F fly ash geopolymer concrete. *Mater. Struct.* **2015**, *48*, 721–731. [CrossRef]
176. Alabi, S.A.; Mahachi, J. Chloride ion penetration performance of recycled concrete with different geopolymers. *Mater. Today Proc.* **2021**, *38*, 762–766. [CrossRef]
177. Duan, P.; Yan, C.; Zhou, W.; Luo, W.; Shen, C. An investigation of the microstructure and durability of a fluidized bed fly ash–metakaolin geopolymer after heat and acid exposure. *Mater. Des.* **2015**, *74*, 125–137. [CrossRef]
178. Marvila, M.T.; Azevedo, A.R.G.; Delaqua, G.C.G.; Mendes, B.C.; Pedroti, L.G.; Vieira, C.M.F. Performance of geopolymer tiles in high temperature and saturation conditions. *Constr. Build. Mater.* **2021**, *286*, 122994. [CrossRef]
179. Choi, Y.C.; Park, B. Effects of high-temperature exposure on fractal dimension of fly-ash-based geopolymer composites. *J. Mater. Res. Technol.* **2020**, *9*, 7655–7668. [CrossRef]
180. Mermerdaş, K.; İpek, S.; Mahmood, Z. Visual inspection and mechanical testing of fly ash-based fibrous geopolymer composites under freeze-thaw cycles. *Constr. Build. Mater.* **2021**, *283*, 122756. [CrossRef]
181. Jin, M.; Wang, Z.; Lian, F.; Zhao, P. Freeze-thaw resistance and seawater corrosion resistance of optimized tannery sludge/metakaolin-based geopolymer. *Constr. Build. Mater.* **2020**, *265*, 120730. [CrossRef]
182. Rashad, A.M.; Sadek, D.M. Behavior of alkali-activated slag pastes blended with waste rubber powder under the effect of freeze/thaw cycles and severe sulfate attack. *Constr. Build. Mater.* **2020**, *265*, 120716. [CrossRef]
183. Canakci, H.; Güllü, H.; Alhashemy, A. Performances of using geopolymers made with various stabilizers for deep mixing. *Materials* **2019**, *12*, 2542. [CrossRef]
184. Mozumder, R.A.; Laskar, A.I. Prediction of unconfined compressive strength of geopolymer stabilized clayey soil using artificial neural network. *Comput. Geotech.* **2015**, *69*, 291–300. [CrossRef]
185. Rios, S.; Ramos, C.; Viana da Fonseca, A.; Cruz, N.; Rodrigues, C. Mechanical and durability properties of a soil stabilised with an alkali-activated cement. *Eur. J. Environ. Civ. Eng.* **2019**, *23*, 245–267. [CrossRef]
186. Zhang, M.; Guo, H.; El-Korchi, T.; Zhang, G.; Tao, M. Experimental feasibility study of geopolymer as the next-generation soil stabilizer. *Constr. Build. Mater.* **2013**, *47*, 1468–1478. [CrossRef]
187. Abdullah, H.H.; Shahin, M.A.; Sarker, P. Use of Fly-Ash Geopolymer Incorporating Ground Granulated Slag for Stabilisation of Kaolin Clay Cured at Ambient Temperature. *Geotech. Geol. Eng.* **2019**, *37*, 721–740. [CrossRef]
188. Odeh, N.A.; Al-Rkaby, A.H.J. Strength, Durability, and Microstructures characterization of sustainable geopolymer improved clayey soil. *Case Stud. Constr. Mater.* **2022**, *16*, e00988. [CrossRef]
189. Jittabut, P. Physical properties and thermal conductivity of soil geopolymer block. *J. Phys. Conf. Ser.* **2019**, *1380*, 012038. [CrossRef]
190. Zain-ul-abdein, M.; Ahmed, F.; Channa, I.A.; Makhdoom, M.A.; Ali, R.; Ehsan, M.; Aamir, A.; Ul Haq, E.; Nadeem, M.; Shafi, H.Z.; et al. Synthesis of Geopolymer from a Novel Aluminosilicate-Based Natural Soil Precursor Using Electric Oven Curing for Improved Mechanical Strength. *Materials* **2022**, *15*, 7757. [CrossRef] [PubMed]
191. Liyana, J.; Al Bakri, A.M.; Hussin, K.; Ruzaidi, C.M.; Azura, A.R. Azura, Effect of Fly Ash/Alkaline Activator Ratio and Sodium Silicate/NaOHRatio on Fly Ash Geopolymer Coating Strength. *Eng. Mater.* **2014**, *594–595*, 146–150.

192. Singh, S.; Kant Sharma, S.; Abdul Akbar, M. Developing zero carbon emission pavements with geopolymer concrete: A comprehensive review. *Transp. Res. Part D Transp. Environ.* **2022**, *110*, 103436. [CrossRef]
193. Ojha, A.; Gupta, L. Comparative study on mechanical properties of conventional and geo-polymer concrete with recycled coarse aggregate. *Mater. Today Proc.* **2020**, *28*, 1403–1406. [CrossRef]
194. Rahman, S.S.; Khattak, M.J. Feasibility of Reclaimed Asphalt Pavement Geopolymer Concrete as a Pavement Construction Material. *Int. J. Pavement Res. Technol.* **2022**. [CrossRef]
195. Flower, D.J.M.; Sanjayan, J.G. Green house gas emissions due to concrete manufacture. *Int. J. Life Cycle Assess.* **2007**, *12*, 282–288. [CrossRef]
196. CIRCULAR-ECOLOGY Embodied Carbon Calculator for Concrete Launched. 2020. Available online: https://circularecology.com/news/embodied-carbon-calculator-for-concrete-launched (accessed on 1 January 2023).
197. Turner, L.K.; Collins, F.G. Carbon dioxide equivalent (CO_2-e) emissions: A comparison between geopolymer and OPC cement concrete. *Constr. Build. Mater.* **2013**, *43*, 125–130. [CrossRef]
198. Heath, A.; Paine, K.; McManus, M. Minimising the global warming potential of clay based geopolymers. *J. Clean. Prod.* **2014**, *78*, 75–83. [CrossRef]
199. Hayden, A. *Ecological Footprint*; Encyclopedia Britannica: Chicago, IL, USA, 2019.
200. GFN. Ecological Footprint. 2022. Available online: https://www.footprintnetwork.org/our-work/ecological-footprint/ (accessed on 2 February 2023).
201. Farhan, N.A.; Sheikh, M.N.; Hadi, M.N.S. Investigation of engineering properties of normal and high strength fly ash based geopolymer and alkali-activated slag concrete compared to ordinary Portland cement concrete. *Constr. Build. Mater.* **2019**, *196*, 26–42. [CrossRef]
202. Diaz-Loya, E.I.; Allouche, E.N.; Vaidya, S. Mechanical properties of fly-ash-based geopolymer concrete. *ACI Mater. J.* **2011**, *108*, 300.
203. Deb, P.S.; Nath, P.; Sarker, P.K. The effects of ground granulated blast-furnace slag blending with fly ash and activator content on the workability and strength properties of geopolymer concrete cured at ambient temperature. *Mater. Des. (1980–2015)* **2014**, *62*, 32–39. [CrossRef]
204. Fang, G.; Ho, W.K.; Tu, W.; Zhang, M. Workability and mechanical properties of alkali-activated fly ash-slag concrete cured at ambient temperature. *Constr. Build. Mater.* **2018**, *172*, 476–487. [CrossRef]
205. Ahmari, S.; Zhang, L.; Zhang, J. Effects of activator type/concentration and curing temperature on alkali-activated binder based on copper mine tailings. *J. Mater. Sci.* **2012**, *47*, 5933–5945. [CrossRef]